

**UNDER A-SALT:**  
**Investigating the role of CosR in Osmotic Stress Response Of**  
*Vibrio parahaemolyticus*

by

Daniel P. Morreale

A thesis submitted to the Faculty of the University of Delaware in partial fulfillment of the requirements for the degree of Honors Bachelor of Science in Biology with a concentration in Cell and Molecular Biology & Genetics with Distinction

Spring 2019

© 2019 Daniel P. Morreale  
All Rights Reserved

**UNDER A-SALT:**  
**Investigating the role of CosR in Osmotic Stress Response Of**  
***Vibrio parahaemolyticus***

by

Daniel P. Morreale

Approved: \_\_\_\_\_  
E. Fidelma Boyd, Ph.D.  
Professor in charge of thesis on behalf of the Advisory Committee

Approved: \_\_\_\_\_  
William Cain, Ph.D.  
Committee member from the Department of Biological Sciences

Approved: \_\_\_\_\_  
Kalmia Kniel Name, Ph.D.  
Committee member from the Board of Senior Thesis Readers

Approved: \_\_\_\_\_  
Earl Lee II, Ph.D.  
Director, University Honors Program

## ACKNOWLEDGMENTS

First and foremost, I would like to thank Professor Boyd for affording me the opportunity to join her lab. From the moment I started working with her, Dr. Boyd has always pushed for the highest quality work feasible and would never settle for less. Her patient mentoring and passion for her work has had an enormous impact on my drive to do the best science possible. As I continue on from the University of Delaware, I am certain that I will rely on the lessons I have learned under her guidance. I would also like to thank Dr. Cain, whom I have had the pleasure of learning from over the last two years. Dr. Cain has shown me the importance of a true passion for learning, and I wish him all the best as his time at the University of Delaware comes to an end and he moves into retirement (though, I have no doubt he will continue to pursue his passion for biology in between Phillies games). Additionally, I would like to extend my gratitude to Dr. Kniel for her support and comments as I have worked to complete this thesis.

During my time in the Boyd Lab, I have had the distinct pleasure of working with four graduate student mentors with vastly different expertise and interests. The first, Mr. Joe Borowski, patiently taught me as I started out on my research career. Drs. Nathan McDonald and Abish Regmi helped me refine my ability to construct and address research questions, as well as build the basic skills required for manuscript writing and effective communication. However, most important to the work presented in this document has been Gwen Gregory. Over the course of this project, Gwen has taken the time to teach me any technique I have wanted to learn and has given me the

freedom and ownership to help determine the direction that this project would take. Two years ago, at the start of my time at the Boyd Lab, she was the first student to take the time to explain her project to me, so I find it fitting I end my undergraduate research career working with her. I would also like to thank each of the remaining members of the Boyd lab: Jess Tague, Kent Kwah, and John Rosenberg. Each of you has helped to make each day in the lab a pleasure and I cannot wait to see what you will all accomplish in your scientific careers.

## TABLE OF CONTENTS

LIST OF TABLES .....	vii
LIST OF FIGURES.....	viii
ABSTRACT .....	xii
1 INTRODUCTION.....	1
1.1 An Introduction to <i>Vibrio</i> .....	1
1.2 <i>Vibrio parahaemolyticus</i> .....	3
1.3 Salt Stress Response in Bacteria.....	5
1.3.1 Uptake of Compatible Solutes.....	8
1.3.2 Biosynthesis of Compatible Solutes.....	10
1.4 Regulation of Compatible Solute Production and Uptake .....	11
1.4.1 Indirect Regulation of Compatible solutes .....	11
1.4.2 Direct regulators of Compatible Solute uptake and biosynthesis .....	12
1.4.3 MarR-type Regulators .....	13
1.5 Aims of this Study .....	15
2 MATERIALS AND METHODS .....	17
2.1 Bioinformatics Analyses .....	17
2.2 Bacterial Strains, Plasmids, And Growth Conditions. ....	17
2.3 Construction of the $\Delta\text{cosR}$ mutant.....	19
2.4 Growth Analysis.....	22
2.5 RNA Extraction and Quantitative Real-Time PCR.....	22
2.6 Protein Expression and Purification .....	23
2.7 <i>E. coli</i> GFP Reporter Assay.....	24
2.8 Electrophoretic Mobility Shift Assay.....	25
2.9 Biofilm assay .....	26
3 RESULTS.....	27
3.1 <i>In silico</i> analysis of <i>V. parahaemolyticus</i> CosR.....	27
3.2 Expression of the Compatible Solute Genes in low salt.....	27
3.3 Growth Analysis of <i>V. parahaemolyticus</i> $\Delta\text{cosR}$ .....	30
3.4 Expression of <i>bcct1</i> and <i>bcct3</i> are regulated by CosR in Low Salt Conditions .....	35

3.5	CosR expression is independent of salt concentration and does not autoregulate .....	39
3.6	CosR represses biofilm formation .....	42
3.7	Distribution of CosR-homologs among the Vibrionaceae .....	43
4	DISCUSSION.....	47
4.1	CosR regulates elements of the osmotic stress response in <i>Vibrio parahaemolyticus</i> .....	47
4.2	CosR is highly conserved and phylogenetically widespread .....	48
4.3	Future works .....	49
	REFERENCES.....	51
A.1	Primers Used in this study .....	64
A.2	Supplementary Figure 1. ....	66

## LIST OF TABLES

Table 1. Bacterial strains and plasmids used in this study. ....	18
Table 2. Compatible solute systems identified in select species of Vibrionaceae. ....	44
Table S1. Primers Used in this Study. ....	64

## LIST OF FIGURES

- Figure 1. Incidence of bacterial food poisoning in 2017 as compared to 2014-2016. While other common food pathogens such as Salmonella, were associated with fewer diagnosed infections in 2017, the incidence of Vibrio infections increased by more than 50%, a trend consistent with data collected over the last two decades. (Marder *et al.*, 2017) ..... 2
- Figure 2. A. In many bacteria, the short-term response to increased osmolarity in the environment involves the uptake of potassium ions. However, as  $K^+$  accumulation in the cell can interfere with a number of cellular processes. This will lead to eventual cell death. B. The long-term response in involves the uptake and biosynthesis of compatible solutes. *V. parahaemolyticus* encodes at least six compatible solute transporters: ProU1, ProU2, and BCCT1-BCCT4, as well as two compatible solute biosynthesis operons: glycine betaine and ectoine. .... 7
- Figure 3. Model of CosR regulation in *V. cholerae*. When this organism is grown in low salt conditions, CosR was shown to activate genes involved in biofilm formation. CosR represses genes involved in motility and the osmotic stress response, specifically the ectoine biosynthesis operon and the BCCT homolog, OpuD (Shikuma *et al.*, 2013). ..... 15
- Figure 4. Workflow for vector construction using Gibson assembly. PCR fragments are ligated together with a digested plasmid, in this case pDS132, using a proprietary mix of exonucleases that generate sticky ends on all of the fragments. After ligation, the assembled vector can be transformed into *E. coli* Dh5 $\alpha$  for propagation. .... 21
- Figure 5. *E. coli* MKH13 GFP-assay. Two plasmids are transformed into this strain. A. The first, shown here as pBBRCosR, encodes the ORF of interest under control of an IPTG-inducible promoter. The addition of IPTG stimulates production of the protein, which is then free to interact with the second vector. B. A second vector encodes a GFP CDS under control of a promoter of interest, in this instance the promoter for the ectoine operon. Transcription from this promoter will produce the GFP protein, which will accumulate in the cell and be quantified after 20 hours of growth. .... 25
- Figure 6. Relative expression of *ectA* and *aspK* in M9G 1% NaCl compared to M9G 3% NaCl in *V. parahaemolyticus* RIMD2210633. Cells were grown to an OD of 0.5, RNA extracted, and qPCR was performed using gene specific primers. Fold changes were calculated using the  $\Delta\Delta C_T$  method and the data was analyzed with a student's t-test. .... 28

- Figure 7. A. Relative expression of *bcct1*, *bcct2*, *bcct3*, and *bcct4* in M9G 1% NaCl compared to M9G 3% NaCl in *V. parahaemolyticus* RIMD2210633. Cells were grown to an OD of 0.5, RNA extracted, and qPCR was performed using gene specific primers. Fold changes were calculated using the  $\Delta\Delta C_T$  method and the data was analyzed with a student's t-test. Depicted is average fold change  $\pm$  1 standard deviation. .... 29
- Figure 8. Relative expression of *bcct1*, *bcct2*, *bcct3*, and *bcct4* in M9G 1% NaCl + 100  $\mu$ M ectoine relative to M9G 1% NaCl. Cells were grown to an OD of 0.5, RNA extracted, and qPCR was performed using gene specific primers. Fold changes were calculated using the  $\Delta\Delta C_T$  method and the data was analyzed with a student's t-test. Depicted is average fold change  $\pm$  1 standard deviation. .... 30
- Figure 9. Growth analyses of *V. parahaemolyticus* RIMD2210633 and  $\Delta$ *cosR* in A. LBS, B. M9G 1% NaCl, and C. M9G 1% NaCl supplemented with 100  $\mu$ M ectoine. As the mutant and wild-type strains grow identically,  $\Delta$ *cosR* shows no growth defects in any of these media. Growth was analyzed over 24 hours with periodic shaking; each point shown in the average OD  $\pm$  1 standard deviation. .... 31
- Figure 10. Ectoine operon expression in  $\Delta$ *cosR* relative to WT. Fold changes were calculated using the  $\Delta\Delta C_T$  method and the data was analyzed with a student's t-test. Expression of the *ectA* and *aspK* increased 1000-fold and 300-fold, respectively, in the  $\Delta$ *cosR* strain. Depicted is average fold change  $\pm$  1 standard deviation..... 32
- Figure 11. *E. coli* MKH13 strains harboring pBBRCosR+pRUPectA and pBBRempty+pRUPectA were grown for 20 hours under inducing conditions, at which point specific fluorescence was calculated. *E. coli* MKH13 pBBRempty+pRUPectA exhibited significantly higher specific fluorescence than *E. coli* MKH13 pBBRCosR+pRUPectA. Statistical analysis was conducted using a student's t-test across two replicates. Depicted is average specific fluorescence  $\pm$  1 standard deviation. .... 33
- Figure 12. A. A schematic of the probes used for EMSA. The promoter region of *ectABCaspK* was divided into three probes: 1A (125 bp), 1B (137 bp), and 1C (106 bp). Probes 1A and 1B overlap by 25 bp, probes 1B and 1C overlap by 20 bp. B. 36 ng of each probe was incubated with purified His-CosR in varying concentrations from 0 to 0.44  $\mu$ M. The DNA-protein mixtures were run on a 6% native polyacrylamide gel for 2 hr, stained, and imaged. .... 35

- Figure 13. Expression of the *bcct* genes in  $\Delta\text{cosR}$  compared to WT. Strains were grown to an OD of 0.5, RNA extracted, and qPCR was performed using gene specific primers. Fold changes were calculated using the  $\Delta\Delta C_T$  method and the data was analyzed with a student's t-test across two replicates. Depicted is average fold change  $\pm$  1 standard deviation. 36
- Figure 14. *E. coli* MKH13 strains harboring (A.) pBBRCosR+pRUP*bcct1* and pBBRempty+pRUP*bcct1* (B.) pBBRCosR+pRUP*bcct3* and pBBRempty+pRUP*bcct3* were grown for 20 hours under inducing conditions, at which point specific fluorescence was calculated. *E. coli* MKH13 pBBRempty+pRUP*bcct1* produced significantly more GFP than *E. coli* MKH13 pBBRCosR+pRUP*bcct1*. For each, statistical significance was calculated using a student's t-test and the depicted plot shows the average specific fluorescence  $\pm$  1 standard deviation. .... 37
- Figure 15. A. The intergenic region immediately upstream of *bcct1* was used for this binding analysis. B. A 179 bp intergenic region upstream of *bcct1*. C. 36 ng of each probe was incubated with purified His-CosR in varying concentrations from 0 to 0.2  $\mu\text{M}$ . ..... 38
- Figure 16. Expression of *cosR* in *V. parahaemolyticus* RIMD2210633 in M9G 3% NaCl relative to M9G 1% NaCl. Cells were grown to an OD of 0.5 in the appropriate media, RNA extracted, and qPCR was performed using gene specific primers. Fold changes were calculated using the  $\Delta\Delta C_T$  method and the data was analyzed with a student's t-test across two replicates. Depicted is average fold change  $\pm$  1 standard deviation. 39
- Figure 17. A. Expression of *cosR* in *V. parahaemolyticus* RIMD2210633 in M9G 1% NaCl with 100  $\mu\text{M}$  ectoine, relative to M9G 1% NaCl. B. Expression of *cosR* in *V. parahaemolyticus* RIMD2210633 in M9G 3% NaCl with 100  $\mu\text{M}$  ectoine, relative to M9G 3% NaCl. Cells were grown to an OD of 0.5 in the appropriate media, RNA extracted, and qPCR was performed using gene specific primers. Fold changes were calculated using the  $\Delta\Delta C_T$  method and the data was analyzed with a student's t-test across two replicates. Depicted is average fold change  $\pm$  1 standard deviation. .... 40
- Figure 18. *E. coli* MKH13 strains harboring pBBRCosR+pRUP*cosR* and pBBRempty+pRUP*cosR* were grown for 20 hours under inducing conditions, at which point specific fluorescence was calculated. Statistical significance was calculated using a student's t-test and the depicted plot shows the average specific fluorescence  $\pm$  1 standard deviation. .... 41

Figure 19. A. A 218 bp intergenic region immediately upstream of *cosR* was used for this binding analysis. B. 36 ng of each probe was incubated with purified His-CosR in varying concentrations from 0 to 0.2  $\mu$ M. .... 42

Figure 20. CosR represses biofilm formation in *V. parahaemolyticus*. Biofilms were grown statically at 37 °C for 24 hours. Biofilm was stained with crystal violet, photographed (A), and quantified by determining the OD<sub>595</sub> (B). CosR produced significantly more biofilm than WT ( $p < 0.01$ )..... 43

Figure 21. Select CosR homologs from seven species were aligned with *M. alcaliphilum* 20Z EctR1. The DNA binding, helix-turn-helix domain defined in EctR1 was annotated for all of the proteins and highlighted in yellow. Additionally, secondary structure was predicted using Ali2. Predicted alpha helices are depicted by blue tubes, predicted beta sheets are depicted by green rectangles. A black line denotes unstructured regions without a predicted structure. Residues conserved across all proteins are highlighted in blue..... 46

Figure 22. A model of the CosR low salt regulon in *V. parahaemolyticus*. In these conditions, CosR represses transcription of the ectoine operon, as well as *bcct1*, *bcct3*, and genes involved in biofilm formation. Additionally, we demonstrate that CosR likely represses biofilm formation in optimal salt conditions..... 47

Figure S1. Genomic context of CosR homologs from select Vibrionaceae strains. A. In *V. parahaemolyticus* *cosR* is divergently transcribed from *bcct3* and found on chromosome 1. This structure is well conserved in many *Vibrio* species. B. In *V. tasmaniensis* a CosR homolog is located on chromosome 2, downstream of the *betIBAchoXWV* operon. C. *A. fischeri* encodes a CosR homolog divergently transcribed from *mntH*, a Mn(II) transport protein. D. The *betIBAproVWX* operon of *V. parahaemolyticus* is highly homologous to the *betIBAchoXWV* operon of *V. tasmaniensis*. Homology was determined with tBLASTx. .... 66

## ABSTRACT

The marine bacterium *Vibrio parahaemolyticus* has evolved multiple strategies for adapting to short- and long-term shifts in osmolarity. One such mechanism involves the uptake and/or biosynthesis of small organic molecules known as compatible solutes. These compatible solutes act to balance the osmolarity of the cell without disrupting important biological processes. *V. parahaemolyticus* is able to uptake compatible solutes through six transport systems: two ABC type transporters named ProU1 and ProU2 and four betaine carnitine choline transporters (BCCTs). Additionally, *V. parahaemolyticus* can biosynthesize glycine betaine and ectoine. Ectoine gene expression was previously shown to be regulated by a MarR-type regulator CosR in *V. cholerae*. In this study, we identify a CosR homologue (VP1906) present in all strains of *V. parahaemolyticus* and characterize its role in the osmotic stress response through the generation of a *cosR* deletion strain. Through quantitative Real-Time PCR (qPCR), we demonstrate that CosR plays a role in regulation of the ectoine biosynthesis genes as well as *bcct1* (VP0456) and *bcct3* (VP1905). Additionally, we show that CosR is able to bind to the promoter regions of these operons, as well as directly repress transcription of the *ectABCaspK* operon *in vitro*. Taken together, these data suggest that CosR is an important global regulator in the osmotic stress response of *V. parahaemolyticus*.

## Chapter 1

### INTRODUCTION

#### 1.1 An Introduction to *Vibrio*

*Vibrio* species are ubiquitous in the marine and estuarine environments and includes multiple species that are known human pathogens. *Vibrio cholerae*, the causative agent of the disease cholera, *V. vulnificus*, the cause of vibriosis and necrotizing fasciitis (Dechet *et al.*, 2008), and *V. parahaemolyticus*, the leading cause of global, bacterial seafood borne gastroenteritis (Nair *et al.*, 2007). Each of these species benefit from warmer waters due to climate change, gaining longer growing seasons and colonizing new ecosystems that were previously non-survivable (McLaughlin *et al.*, 2009; Vezzulli *et al.*, 2016). As such, human infections by *Vibrio* species are increasing in frequency in the United States, and have increased by over 50% in 2017, as compared to the previous two years (Fig. 1) (Marder *et al.*, 2017). Commonly, these infections are a result of food that has been improperly handled and prepared to an inadequate temperature to ensure the bacteria are killed. The trend in increased *Vibrio* infections has continued over the last two decades.

While life-threatening *Vibrio* infections are uncommon in United States, recent weather events on the east coast have led to flooding of both sea water and freshwater, increasing vectors of infection (Rhoads, 2006). Post hurricane Katrina and Rita, levels of *Vibrio* spp. were found to be significantly higher in inland lakes than before the storms hit (Nigro *et al.*, 2011), and two cases of cholera were reported to the CDC

(Balter *et al.*, 2006). Additionally, in the last year, epidemics caused by *V. cholerae* have occurred globally, including Yemen, Nigeria, Zimbabwe, and Algeria.

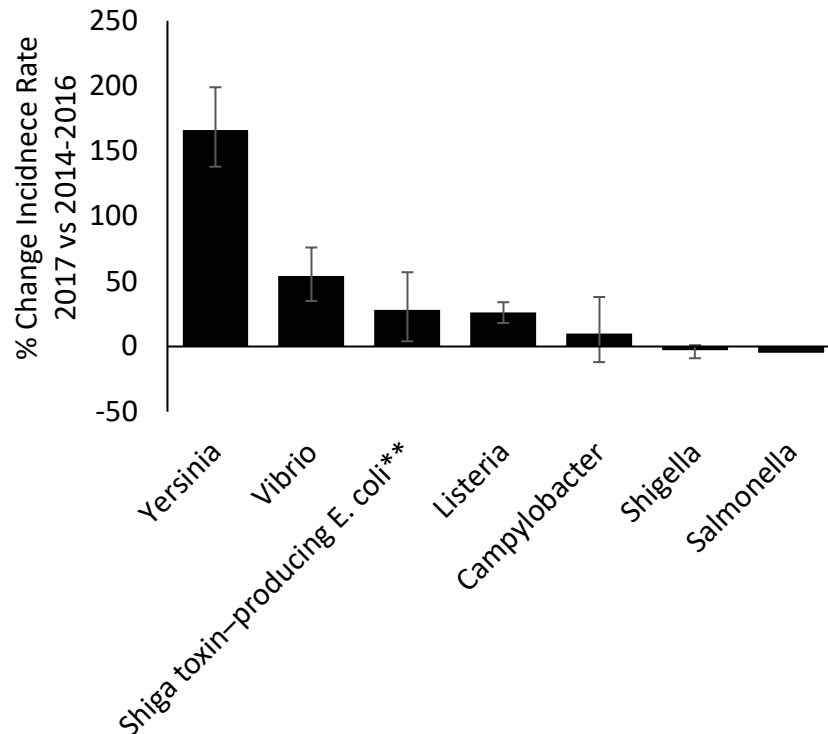


Figure 1. Incidence of bacterial food poisoning in 2017 as compared to 2014-2016. While other common food pathogens such as Salmonella, were associated with fewer diagnosed infections in 2017, the incidence of Vibrio infections increased by more than 50%, a trend consistent with data collected over the last two decades. (Marder *et al.*, 2017)

It is important to note that, in spite of the lethality of some species, non-pathogenic vibrios play a critical role in nutrient cycling, including fixing free nitrogen and the degradation of chitin the second most abundant polymer (Colwell, 2006).

Additionally, a number of *Vibrio* species have evolved commensal relationships with many marine mammals, fish, and shellfish (Colwell, 2006; Romalde *et al.*, 2014).

## 1.2 *Vibrio parahaemolyticus*

Recovered from brackish and marine environments as well as oyster and human hosts, *V. parahaemolyticus* is a human pathogen which causes acute gastroenteritis, the symptoms of which include nausea, diarrhea, headache, and a low fever. Frequently infecting humans through the consumption of raw seafood, the infection self-limits, and the patient typically recovers without issue, unless an underlying health condition is present (Su and Liu, 2007). Since 2000, the United States has experienced four outbreaks of *V. parahaemolyticus* in 2006, 2012, 2013, and 2018; all of which were non-fatal (Balter *et al.*, 2006; Haendiges *et al.*, 2014; Marder *et al.*, 2017).

*V. parahaemolyticus* was first identified in 1950 in Japan, after 272 people became ill, and 20 died, from eating contaminated sardines (FUJINO *et al.*, 1953). In early 1996, a new serogroup of *V. parahaemolyticus* was identified during an outbreak in Calcutta, India (Nair *et al.*, 2007). It was later discovered that 50% to 80% of recovered strains during the outbreak belong to this emerging group, named the O3:K6 serotype, (Okuda *et al.*, 1997). It is believed that O3:K6 arose before its identification in Calcutta, possibly as early as 1983 in Japan, where it evolved from a non-pathogenic strain (Nair *et al.*, 2007). Since the characterization of this serotype, it has been recovered worldwide and from waters previously thought too cold to support growth of *V. parahaemolyticus*, including those around Alaska and Southern Chile (González-Escalona *et al.*, 2005; McLaughlin *et al.*, 2005).

Pathogenicity in *V. parahaemolyticus* is modulated by the presence or absence of a type 3 secretion system (T3SS). Type 3 secretion systems are multicomponent, extracellular structures that facilitate the secretion and injection of virulence factors into surrounding cells (Makino *et al.*, 2003; Park *et al.*, 2004). These secretion systems are further divided into two subtypes. The first of which, T3SS-1, is present in all isolates and is considered essential for survival by allowing the bacterium to lyse surrounding cells for nutrients (Burdette *et al.*, 2008). The second subtype T3SS-2 has been identified in clinical isolates only and is located on a pathogenicity island (Makino *et al.*, 2003; Meador *et al.*, 2007). Although recent data suggest that the T2SS-2 systems are present within a novel Tn-7-like transposon that has co-opted a mini CRISPR-Cas system for mobility (McDonald *et al.*, 2019).

*V. parahaemolyticus* has to cope with various biotic and abiotic stresses during its life cycle. Biotic stresses include challenge by host immune response, which can be coped with through the formation of biofilms, or attack by lytic bacteriophages, which are ubiquitous in all environments, can be managed by CRISPR-Cas systems (Costerton *et al.*, 1999; McDonald *et al.*, 2019).

Abiotic stresses include shifting temperatures, pH, and salinities of the environment (Whitaker *et al.*, 2010). If grown at an optimal salinity of approximately 3% NaCl, *V. parahaemolyticus* can easily survive variable pH and temperature in the environment through the upregulation of general stress response genes including *cadA*, a decarboxylase, *rpoE*, an RNA polymerase sigma factor (Merrell and Camilli, 1999; Whitaker *et al.*, 2010; Haines-Menges *et al.*, 2014).

The larger threat to *V. parahaemolyticus* is the osmolarity of the environment. Salinities can range from 3.5 % in the open ocean, to ~1% in hosts, and as high as 6%

in tidal waters. While *V. parahaemolyticus* is a moderate halophile, salinities above or below an optimal range can severely hinder the general stress response critical for responding to shifts in pH and temperature (Whitaker *et al.*, 2010). If the shift in salinity is brief, the cell can cope via the uptake or release of K<sup>+</sup> ions (Csonka, 1989; Oren, 2008). This is the predominant short-term strategy for many bacteria. However, as the accumulation of intracellular potassium ions will eventually become toxic to the bacterium, very few organisms use it as the sole method of osmoadaptation (Roberts, 2004). A second, more sustainable method of adjusting osmolarity is required, which involves the uptake and biosynthesis of compatible solutes.

### 1.3 Salt Stress Response in Bacteria

Bacteria encounter a broad range of osmolarities in the environment to which they must be able to quickly respond. Shifting osmolarity causes a flux of water across the membrane, either in to or out of the cell, based on the turgor pressure of the cell. Either of these can lead to cell death. To combat these challenges, bacteria have evolved two, distinct phases of the osmotic stress response: the short-term, salt-in-the-cytoplasm response (Galinski and Trüper, 1994) and secondly the long term response acquisitions of compatible solutes (Kempf and Bremer, 1998) (Fig. 2)

The short-term response was originally characterized in *Halobacteriaceae*, a halophilic family of Archaea, that was shown to have the ability to accumulate intracellular ions to 7 M (Lanyi, 1974; Galinski and Trüper, 1994). In *Escherichia coli*, the cell will uptake potassium ions in an attempt to balance the turgor pressure of the cell (Kempf and Bremer, 1998) (Fig. 2A). However, as the K<sup>+</sup> accrues in the cell, the strong positive charge on these cations can damage important molecules and impede cellular processes. To mitigate this, bacteria begin to synthesize organic

anions, such as glutamate, a measurable increase in which can be seen after one minute in up-shocked in *E. coli* (Kempf and Bremer, 1998). This response that is dependent on the intracellular K<sup>+</sup> concentration (Kempf and Bremer, 1998).

Potassium and glutamate ions accumulating in the cells is believed to trigger the conversion to the long-term response mechanism: the uptake and biosynthesis of compatible solutes (Epstein, 1986; Booth and Higgins, 1990). Compatible solutes are small, organic compounds that can balance the osmolarity of the cell without impacting cellular processes or biological molecules, i.e. they do not directly interact with proteins and nucleic acids, and typically are uncharged (Kempf and Bremer, 1998; Poolman and Glaasker, 1998). In fact, these compounds can support the creation of protective hydration shells around sensitive proteins and nucleic acids (Yancey, 2004). Furthermore, these compounds can act to increase the free water in the cell, allowing for continued cell growth and division under adverse environmental conditions (Cayley *et al.*, 1992; Record *et al.*, 1998).

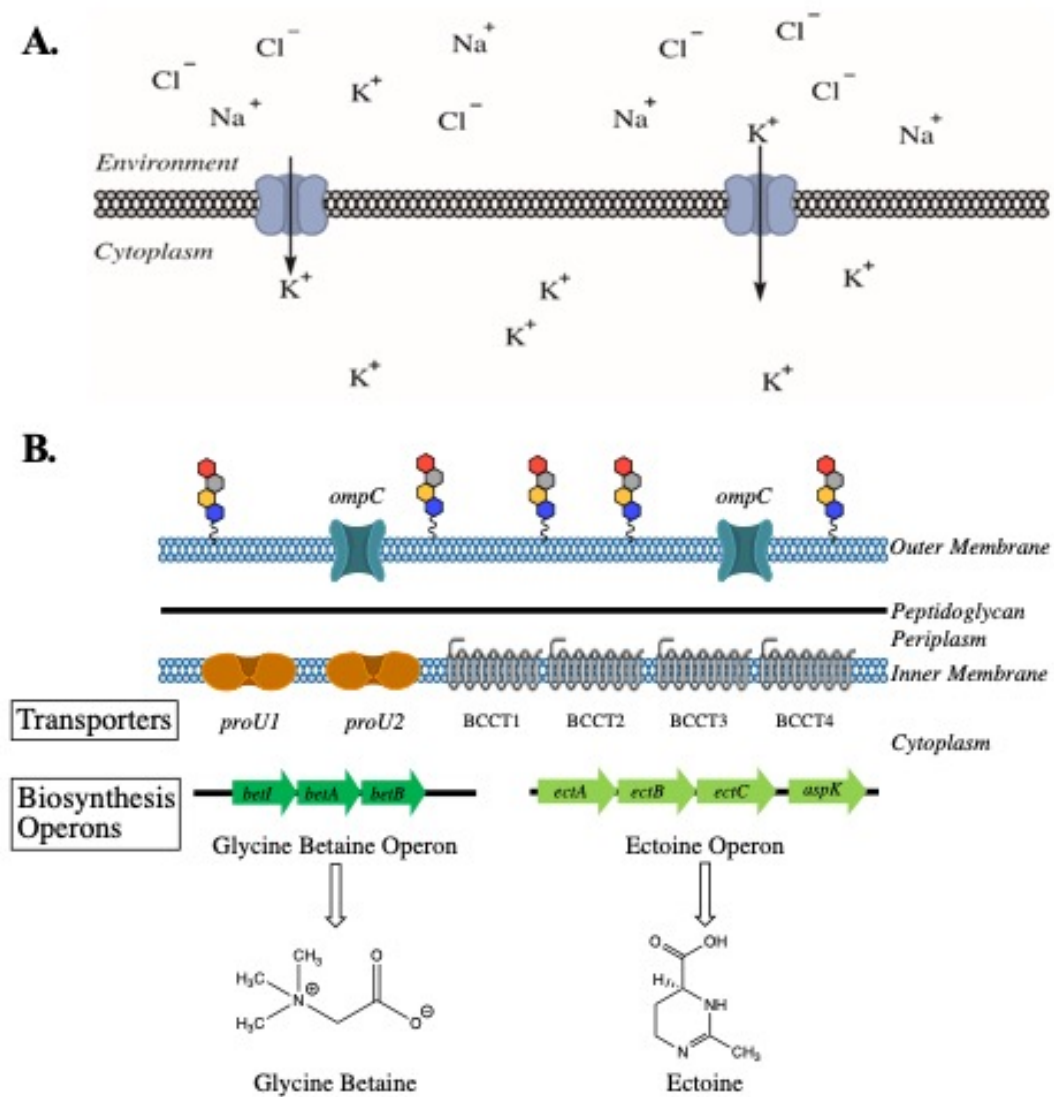


Figure 2. A. In many bacteria, the short-term response to increased osmolarity in the environment involves the uptake of potassium ions. However, as  $K^+$  accumulation in the cell can interfere with a number of cellular processes. This will lead to eventual cell death. B. The long-term response involves the uptake and biosynthesis of compatible solutes. *V. parahaemolyticus* encodes at least six compatible solute transporters: ProU1, ProU2, and BCCT1-BCCT4, as well as two compatible solute biosynthesis operons: glycine betaine and ectoine.

Compatible solutes can be sugars, polyols, and amino acids, or derivatives of any of these species, as well as quaternary amines (da Costa *et al.*, 1998; Poolman and Glaasker, 1998). This can include trehalose (sugar), glycerol (polyol), proline, glutamine (amino acids), carnitine (quaternary amine), ectoine (amino acid derivative), glycine betaine, and numerous other compounds.

### 1.3.1 Uptake of Compatible Solutes

Bacteria will preferentially uptake compatible solutes from the environment as it is energetically favorable to *de novo* production (Kempf and Bremer, 1998; Ventosa *et al.*, 1998; Oren, 1999). In order to accomplish this, *Bacteria* and *Archaea* have osmoregulated transporters that are able to acquire specific compatible solutes from the surrounding environment (Youssef *et al.*, 2014). One such family of transporter is the betaine-carnitine-choline transporter (BCCT), an integral membrane protein with 12 transmembrane passes (Ziegler *et al.*, 2010). This transporter was originally identified in *E. coli*, where it is known as BetT, and transports choline with high affinity (Lamark *et al.*, 1991). A second BCCT family protein, CaiT, has been identified in *E. coli*, and numerous homologs have been observed in diverse bacterial genomes such as *Vibrio cholerae* as well as Gram-positive species such as *Bacillus subtilis* (Eichler *et al.*, 1994; Kappes *et al.*, 1996; Peter *et al.*, 1996; Kapfhammer *et al.*, 2005). High osmolarity has been shown to induce the production of BCCTs (Kappes *et al.*, 1996; Ongagna-Yhombi *et al.*, 2015). These transporters operate through one of three forces: (1) sodium-motive-force-driven, (2) proton-motive-force-driven, or (3) substrate-product antiport (Ziegler *et al.*, 2010). The first two of these involve the use of a chemical gradient to facilitate the binding and intake of surrounding compatible solutes. Substrate-product antiport is used very rarely and

relies the substrate exchange to power up-take. Members of the BCCT family of proteins are able to transport a wide array of substrates including quaternary amines, sugars, amino acids, and amino acid derivatives, yet any given BCCT will only be able to transport a small subset of what is theoretically possible (Ziegler *et al.*, 2010; Ongagna-Yhombi *et al.*, 2015).

In addition to the BCCTs, bacteria can use ATP-Binding Cassette (ABC) transporters that are osmoregulated and able to facilitate the uptake of compatible solutes into the cell (Eitinger *et al.*, 2011). ABC transporters are multimeric complexes characterized by three domains including a transmembrane domain, nucleotide binding domain, and substrate binding domain. In addition, those which are osmoregulated, such as OpuC from *Pseudomonas syringae* have been shown to have an additional pair of domains known as cystathionine- $\beta$ -synthase (CBS), which is critical to osmosensing (Chen and Beattie, 2007). Members of this family uptake compatible solutes, such as the ProU of *E. coli* and OpuC of *P. syringae* (Chen and Beattie, 2007; Gul and Poolman, 2013).

*V. parahaemolyticus* has evolved numerous compatible solute transport systems including two ABC transporters named ProU1 and ProU2, named after a homolog in *E. coli* K12 (Naughton *et al.*, 2009). Additionally, *V. parahaemolyticus* encodes four BCCTs named BCCT1 (VP1456), BCCT2 (VP1723), BCCT3 (VP1905) and BCCT4 (VPA0356), each of which transports specific compatible solutes with different affinities (Naughton *et al.*, 2009; Ongagna-Yhombi *et al.*, 2015). BCCT1 was shown to transport betaine, proline, choline, and ectoine; BCCT2 was shown to transport glycine betaine, choline, and proline; and BCCT3 and BCCT4 were shown to transport glycine betaine (Ongagna-Yhombi *et al.*, 2015).

### 1.3.2 Biosynthesis of Compatible Solutes

If unable to uptake them from the environment, bacteria biosynthesize a number of compatible solutes. The most common compatible solute produced by halophilic phototrophs is glycine betaine (Imhoff, 1986). Production of glycine betaine is a two-step, oxidation reaction based on precursory choline (a compatible solute in its own right for some bacterial species). Choline dehydrogenase and betaine-aldehyde dehydrogenase, encoded by *betA* and *betB* respectively, are responsible for these reactions. These genes are in an operon with genes encoding ProU2 in all *Vibrio* species that can biosynthesize glycine betaine (Naughton *et al.*, 2009; Ongagna-Yhombi and Boyd, 2013; Ongagna-Yhombi *et al.*, 2015).

Aerobic heterotrophs preferentially produce the compatible solute ectoine (Ventosa *et al.*, 1998). Production of ectoine is true *de novo* biosynthesis as the precursor, aspartic acid can be produced by the cell. It is converted into ectoine through the action of EctA, EctB, and EctC, encoded in a single operon that is conserved across bacteria (Louis and Galinski, 1997; Kuhlmann and Bremer, 2002). This operon (*ectABC*) may also contain an aspartokinase gene (*asp*) (Vargas *et al.*, 2008; Lo *et al.*, 2009; Pastor *et al.*, 2010; Schwibbert *et al.*, 2011). Alternatively the final product of these reactions can be converted into 5-hydroxyectoine through the activity of an additional enzyme, EctD (Bursy *et al.*, 2007).

In addition to these two compatible solutes, species have been identified that can produce proline as well as trehalose (Severin *et al.*, 1992). Trehalose biosynthesis genes are commonly identified in Gram-positive species belonging to *Bacillus* and *Actinomyces* (Severin *et al.*, 1992). However, as trehalose is a sugar that can be used for metabolism, biosynthetic and metabolic pathways must be highly regulated by osmolarity dependent switches (Kempf and Bremer, 1998).

*V. parahaemolyticus* encodes two compatible solute biosynthesis systems (Naughton *et al.*, 2009). The first biosynthesis cluster present on chromosome 1, is responsible for the production of ectoine, and is encoded by the *ectABCaspK* operon (Naughton *et al.*, 2009). Ectoine is essential for growth in high salt minimal media, where no other compatible solutes are available, as it can be produced *de novo* from aspartic acid (Ongagna-Yhombi and Boyd, 2013). The second operon, *betIBA*, allows for production of glycine betaine and is present in chromosome 2. These genes are arranged in an operon with the *proVWX* genes (ProU2) (Naughton *et al.*, 2009). Both glycine betaine and ectoine are *bona fide* compatible solutes in *V. parahaemolyticus*, as the bacterium is unable to utilize them as a carbon source (Ongagna-Yhombi and Boyd, 2013).

#### **1.4 Regulation of Compatible Solute Production and Uptake**

As with all bacterial stress responses, the osmotic stress response of bacteria is a highly regulated process. Regulation occurs at both directly and indirectly and is modulated by exogenous compatible solutes, proteins, and post-translational modification.

##### **1.4.1 Indirect Regulation of Compatible solutes**

Expression of the ProU (ABC family) transporter is dependent on osmolarity in *E. coli* and *V. vulnificus*. In both species, ProU uptakes glycine betaine with high affinity, as well as choline in *V. vulnificus* (Gul and Poolman, 2013; Rao *et al.*, 2013). In both, this transporter was significantly induced by increased osmolarity (Lucht and Bremer, 1994; Rao *et al.*, 2013). Additionally, in *Salmonella typhimurium*, the regulation of the ProU is based on the accumulation of cytosolic potassium ions, the

first cellular response to increased osmotic stress (Sutherland *et al.*, 1986; Gowrishankar and Manna, 1996). BCCTs are regulated by osmolarity in much the same way. In *V. parahaemolyticus*, three of the four BCCT genes (with the exception BCCT2) are induced by up-shock into high salt (Ongagna-Yhombi and Boyd, 2013).

Similarly, the biosynthesis operons of many bacteria are under indirect regulation by factors beyond salinity. In *Chromohalobacter*, the addition of glycine betaine to growth media repressed the ectoine genes, as these species preferentially increased uptake of the exogenous compatible solute (Vargas *et al.*, 2006). The addition of choline to the growth media of cold-stressed *V. anguillarum* also repressed expression of ectoine genes (Ma *et al.*, 2017). Modulation in *betIBA* levels in *E. coli* and *Acinetobacter baylyi* can be observed with the addition of choline, leading to an increase in operon expression (Eshoo, 1988; Scholz *et al.*, 2016).

Ectoine and glycine betaine biosynthesis is additionally regulated by salt in the media. In *V. vulnificus*, high osmolarity was shown to induce the *betIBA* genes (Rao *et al.*, 2013). Numerous species showed similar regulatory patterns including *E. coli*, and *A. baylyi*, both of which showed increased *betIBA* transcript levels in the presence of increased NaCl (Eshoo, 1988; Scholz *et al.*, 2016). The ectoine genes of *V. parahaemolyticus* are induced by increased NaCl, indicative of osmotic regulation (Ongagna-Yhombi and Boyd, 2013).

#### **1.4.2 Direct regulators of Compatible Solute uptake and biosynthesis**

Direct regulation of the compatible solute transporters has been shown in a number of species. In *E. coli* the ProU was shown to be regulated by a nucleoid associated protein, H-NS, which is capable of altering the secondary structure of DNA (Khodr *et al.*, 2015). Additionally, the *betIBAprOXWV* operon regulated by two

proteins, LuxR and BetI, which participate in an autoregulatory loop (van Kessel *et al.*, 2015). In both *E. coli* and *A. baylyi*, BetI regulates the *betIBA* operon (Lamark *et al.*, 1996; Scholz *et al.*, 2016). Additionally, BetI regulates BetT of *E. coli*, which is divergently transcribed from the *betIBA* operon (Lamark *et al.*, 1996). BetI is a member of the TetR family of proteins and is comprised of an N-terminal DNA binding domain, act as a dimer, and interacts with one or more ligands that can modulate protein binding (Cuthbertson and Nodwell, 2013).

The regulatory network of the ectoine biosynthesis genes also includes a number of global and local regulators. *Methylobacterium alcaliphilum* 20Z, a halotolerant methanotroph, encodes EctR1, a regulatory protein shown to bind to the *ectABC* promoter and repress transcription of the ectoine biosynthesis genes (Mustakhimov *et al.*, 2010). Homologues to EctR1 have been identified in a diverse sampling of halotolerant methanotrophs, all of which seem to function through the same mechanisms (Reshetnikov *et al.*, 2011). In *V. cholerae*, regulation of the ectoine genes is accomplished by CosR, which affects transcription of both the ectoine operon and a BCCT homolog, OpuD (Shikuma *et al.*, 2013). EctR1 and CosR are both MarR type regulators (Mustakhimov *et al.*, 2010; Shikuma *et al.*, 2013). Regulation of the ectoine biosynthesis operon in *V. parahaemolyticus* is unknown.

### 1.4.3 MarR-type Regulators

Multiple antibiotic resistance, or MarR, type regulators were first identified and characterized in *E. coli*, and are important regulators of a number of cellular responses, typically in response to a change in the external environment (Cohen *et al.*, 1993; Sulavik *et al.*, 1995; Perera and Grove, 2010). Since the first protein was identified, over 12,000 have been annotated across diverse bacterial and archaeal

genomes (Finn *et al.*, 2010; Perera and Grove, 2010). Members of this family usually function through homodimerization and all contain a conserved helix-turn-helix DNA binding motif (Alekshun *et al.*, 2001; Hong *et al.*, 2005; Ellison and Miller, 2006; Chang *et al.*, 2010; Perera and Grove, 2010). MarR complexes interact with ligands in a variety of ways. Primarily, tight binding of small phenolic compounds to one or both of the MarR proteins can inhibit dimerization or displace domains that block the DNA binding domains, thereby abolishing the ability of the complex to bind DNA (Hong *et al.*, 2005; Saridakis *et al.*, 2008; Chang *et al.*, 2010; Perera and Grove, 2010; Brier *et al.*, 2012).

DNA binding sites are pseudopalindromic sequences comprised of 16-20 bp inverted repeats (Perera and Grove, 2010). Individual members of the MarR family can act as either activators, repressors, or both; the effect of DNA binding on regulated genes is largely depending on the binding site. Binding close to the promoter of a gene can inhibit binding of RNA polymerase and transcription factors, inactivating the target gene (Cohen *et al.*, 1993). However, when MarR-type proteins bind further upstream of a target gene they can serve to activate transcription of the ORF (Fiorentino *et al.*, 2007; Di Fiore *et al.*, 2009; Perera and Grove, 2010).

A study in *V. cholerae* identified a MarR-type regulator that also acts to modulate the expression of the ectoine operon, as well as a number of other genes. This protein, named CosR (Compatible Solute Regulator), was found to have a regulon of approximately 30 genes with wide-ranging functions including biofilm formation, virulence, and osmotic stress response regulation (Fig. 3, Shikuma *et al.*, 2013). In the context of the osmotic stress response, CosR repressed the transcription of the ectoine biosynthesis operon in low salt conditions, and microarray data

suggested that CosR repressed OpuD, the BCCT homologue that is divergently transcribed from *cosR* in *V. cholerae* (Shikuma *et al.*, 2013).

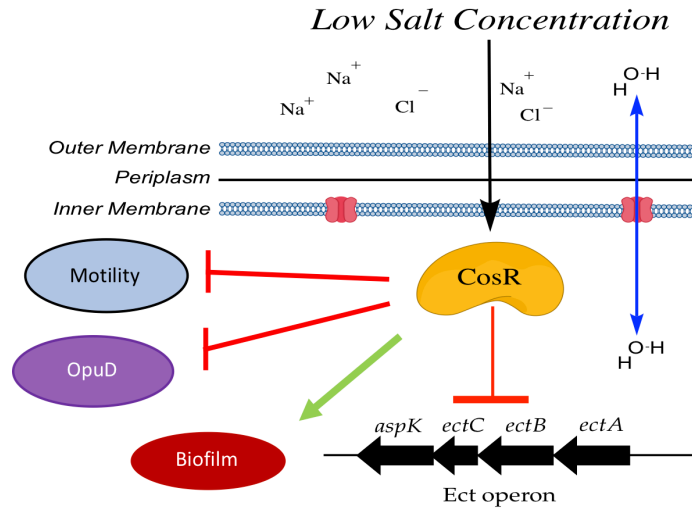


Figure 3. Model of CosR regulation in *V. cholerae*. When this organism is grown in low salt conditions, CosR was shown to activate genes involved in biofilm formation. CosR represses genes involved in motility and the osmotic stress response, specifically the ectoine biosynthesis operon and the BCCT homolog, OpuD (Shikuma *et al.*, 2013).

### 1.5 Aims of this Study

Here we characterize the functions of the CosR homologue VP1906 in *V. parahaemolyticus*. Using a combination of *in vitro* and *in vivo* assays, we demonstrate that CosR binds the regulatory regions of a number of genes critical to the osmotic stress response of this bacteria. Specifically, we investigated the role of CosR in the regulation of the *ectABCaspK* operon as well as the regulation of the *bcct* genes. To accomplish this, we generated a deletion strain, harboring a truncated *cosR* locus for use in RNA extraction and quantitative Real-Time (qPCR) to determine difference in

transcript levels of genes of interest. We purify CosR for use in DNA-binding assays to demonstrate direct, *in vitro* interactions between CosR and the promoter regions of our target operons. This was followed by *in situ E. coli* GFP-assays. Overall, our data suggest that CosR is an important regulator in low salt conditions.

## Chapter 2

### MATERIALS AND METHODS

#### 2.1 Bioinformatics Analyses

The characterized CosR from *V. cholerae* was used as a query in a BLAST *V. parahaemolyticus* (taxid: 665) genome databases. To determine the conservation of primary and secondary structures among strains, six diverse strains were aligned with *V. parahaemolyticus* CosR and *M. alcaliphilum* 20Z EctR1 using ClustX and MEGA7 (Thompson *et al.*, 1994; Kumar *et al.*, 2016). Secondary structure was predicted using Ali2D, and mapped to the multiple sequence alignment (Jones, 1999; Nugent and Jones, 2009; Zimmermann *et al.*, 2018)

Seed sequences from the *V. parahaemolyticus* proteins were used as seeds for BLASTp analyses: EProV (NP\_987105.1), PProX (NP\_800621.1), BCCT2 (NP\_798102.1), EctA (NP\_798101.1), and BetI (NP\_800624.1). For each, a homologous ORF in the strain of interest is considered “presence” of the system, and lack of homology is considered “absence” of the system.

To predict putative ligand binding sites, a 3-D rendering of the structure of CosR was generated using the SWISS-MODEL, a homology modelling tool, which also predicts putative ligand binding sites (Guex *et al.*, 2009; Bienert *et al.*, 2017; Waterhouse *et al.*, 2018). All programs were run with default settings.

#### 2.2 Bacterial Strains, Plasmids, And Growth Conditions.

All bacterial strains and plasmids used in this study are listed in Table 1. All *V. parahaemolyticus* strains were grown aerobically at 37 °C in Luria Bertani (LB) broth, with a final NaCl concentration adjusted to 1% NaCl or 3% NaCl, as necessary. If

required, 100  $\mu$ M ectoine was added to the media. When necessary chloramphenicol (Cm), kanamycin (Kan) and tetracycline (Tet) were used at a concentration of 12.5  $\mu$ g/mL, 40  $\mu$ g/mL, and 6.25  $\mu$ g/mL, respectively. All *E. coli* strains were grown with media containing 1% NaCl. *E. coli*  $\beta$ 2155  $\lambda$ pir strains were grown in LB supplemented with 0.3 mM diaminopimelic acid (DAP). All nucleic acid manipulations were confirmed by sequencing.

Table 1. Bacterial strains and plasmids used in this study.

Strain or Plasmid	Genotype/Strain Characteristics
<i>V. parahaemolyticus</i>	
RIMD2210633	O3:K6 clinical isolate
$\Delta$ cosR	RIMD2210633 $\Delta$ cosR (VP1906)
$\Delta$ rpoS	RIMD2210633 $\Delta$ rpoS (VP2553)
<i>E. coli</i>	
DH5 $\alpha$ $\lambda$ pir	$\Delta$ lac pir
$\beta$ 2155 $\lambda$ pir	$\Delta$ dapA:erm pir
DH5 $\alpha$ $\lambda$ pir pDS $\Delta$ cosR	DH5 $\alpha$ $\lambda$ pir containing pDS $\Delta$ cosR
$\beta$ 2155 $\lambda$ pir pDS $\Delta$ cosR	$\beta$ 2155 containing pDS $\Delta$ cosR
BL21	Protein expression strain
BL21 pET-CosR	BL21 harboring IPTG-inducible, CosR expression vector
MKH13	MC4100 derived strain deficient in CS uptake and biosynthesis genes
MKH13 pBBRCosRpRUPectA	MKH13 harboring pBBRCosR and pRUPectA
MKH13 pBBRCosRpRUPbcct1	MKH13 harboring pBBRCosR and pRUPbcct1
MKH13 pBBRCosRpRUPbcct3	MKH13 harboring pBBRCosR and pRUPbcct3
MKH13 pBBRemptypRUPectA	MKH13 harboring pBBR1MCS empty vector and pRUPectA
MKH13 pBBRemptypRUPbcct1	MKH13 harboring pBBR1MCS empty vector and pRUPbcct1
MKH13 pBBRemptypRUPbcct3	MKH13 harboring pBBR1MCS empty vector and pRUPbcct3

Strain or Plasmid	Genotype/Strain Characteristics
Plasmids	
pDS132	Suicide plasmid; Cm <sup>r</sup> ; SacB
pDSΔcosR	pDS132 containing a truncated <i>cosR</i>
pET-28a (+)	Expression vector, LacZ, 6x His-tag; Km <sup>r</sup>
pET-cosR	CosR pET-28a (+) expression vector
pRU1064	GFP Expression Vector, Tet <sup>r</sup>
pRUP <i>ectA</i>	pRU1064 containing the promoter region of <i>ectA</i>
pRUP <i>cosR</i>	pRU1064 containing the promoter region of <i>cosR</i>
pRUP <i>bcct1</i>	pRU1064 containing the promoter region of <i>bcct1</i>
pRUP <i>bcct3</i>	pRU1064 containing the promoter region of <i>bcct3</i>
pBBR1MCS	Lactose inducible expression vector Amp <sup>r</sup>
pBBRCosR	pBBR1MCS harboring the <i>cosR</i> CDS
pBBRopaR	pBBR1MCS harboring the <i>opaR</i> CDS

### 2.3 Construction of the Δ*cosR* mutant

A Gibson Assembly protocol (Gibson *et al.*, 2009; Gibson, 2011) was used to generate a truncated, non-functional *cosR* gene, followed by allelic exchange to generate a *cosR* (VP1906) deletion mutant in *V. parahaemolyticus* RIMD2210633. Primers used are listed in Appendix Table S1. The Gibson assembly was first used to generate pDSΔ*cosR*, the pDS132 plasmid harboring the 993-bp truncated *cosR* locus (Fig. 4). pDS132, a suicide vector conferring resistance to chloramphenicol, as well as sensitivity to sucrose (Philippe *et al.*, 2004), was linearized with SacI. A PCR was performed on *V. parahaemolyticus* DNA using primers with homology to both pDS132 and the bacterium. These fragments could then be assembled with

linearized pDS132, yielding pDS $\Delta$ *cosR*. This vector was then transformed into *E. coli* DH5 $\alpha$   $\lambda$ *pir* using a CaCl<sub>2</sub> transformation protocol.

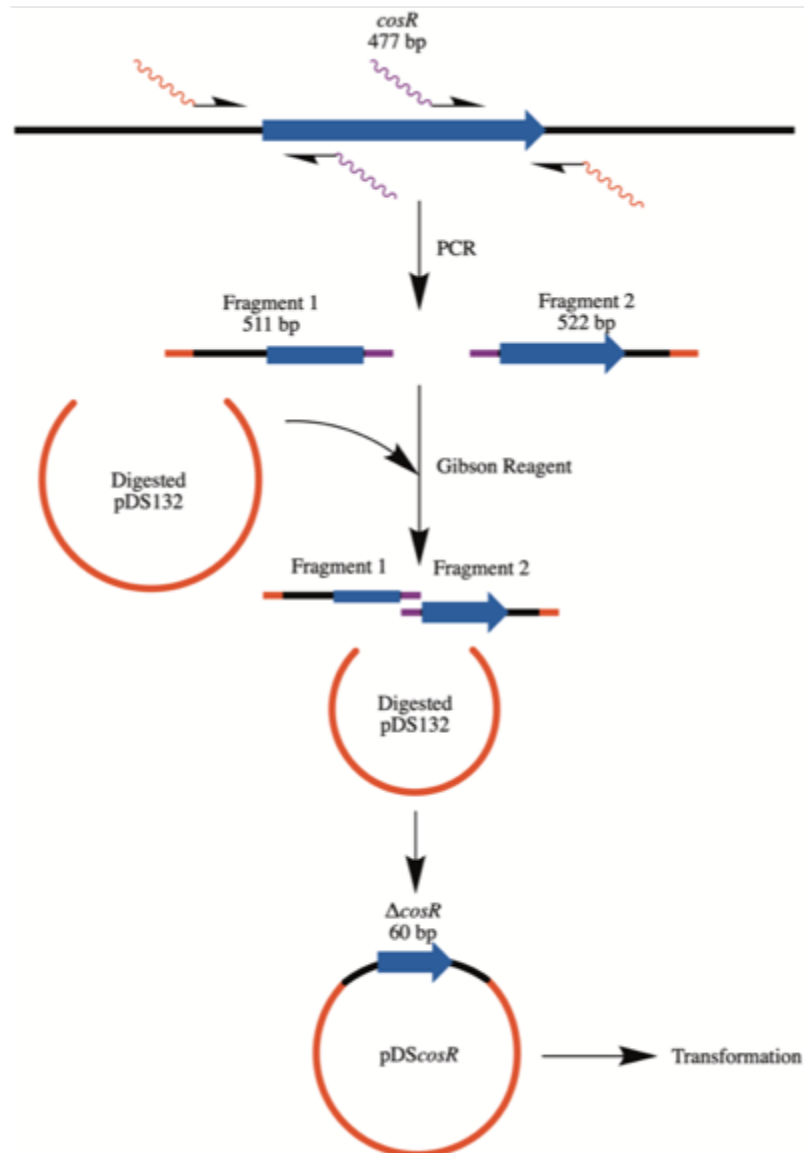


Figure 4. Workflow for vector construction using Gibson assembly. PCR fragments are ligated together with a digested plasmid, in this case pDS132, using a proprietary mix of exonucleases that generate sticky ends on all of the fragments. After ligation, the assembled vector can be transformed into *E. coli* Dh5 $\alpha$  for propagation.

After overnight incubation, pDS $\Delta$ *cosR* was purified from cultures, and transformed into *E. coli*  $\beta$ 2155  $\lambda$ *pir*. The plasmid was then conjugated to *V. parahaemolyticus* RIMD2210633 on an agar plate supplemented with DAP. After overnight growth, the cells were collected and plated onto LB plates with 3% NaCl (LBS). Single crossovers were identified using colony PCR. A colony positive for the single crossover was selected and grown aerobically at 37°C without antibiotics. The culture was serially diluted and plated onto LBS plates containing sucrose. Colonies were screened using PCR with the VP1906A/D primer pairs. Colonies which were positive for the truncated, 60-bp *cosR* were passaged on LBS plates.

#### **2.4 Growth Analysis.**

M9-minimal media supplemented with 20mM glucose and 1% NaCl (M9G 1% NaCl) was inoculated and grown aerobically overnight. The cells from this culture were pelleted at 11,000xg for 5 min, washed in PBS, and 5  $\mu$ L added to a 96-well plate containing 195  $\mu$ L of M9G with 1% or 3% NaCl.

Cells used in analyses with added ectoine were grown overnight in M9G 1% NaCl supplemented with 100  $\mu$ M ectoine. As above, these cells were then pelleted and suspended in fresh media containing the supplemented ectoine and salt. Growth was measured over 24 hours at 37°C with periodic shaking. Optical densities were measured at 595 nm (OD<sub>595</sub>) using a Magellan Plate reader.

#### **2.5 RNA Extraction and Quantitative Real-Time PCR.**

Cells were grown aerobically at 37 °C, in the applicable media to mid-exponential phase (OD<sub>600</sub> 0.5). RNA was extracted as previously described (Kalburge *et al.*, 2017). 1 mL of culture was pelleted, and RNA extracted using Trizol, following

the manufacturer's protocol. Total nucleic acid in the sample was then measured using Nanodrop, after which the samples were treated with DNase, followed by heat inactivation of the enzyme as per manufacturer's protocol. Final RNA concentration was quantified, again using Nanodrop. 500 ng of RNA were used for cDNA synthesis using SSIV reverse transcriptase, following manufacturer's protocol.

Synthesized cDNA was diluted 1:25, and PowerUp SYBR master mix was used for qPCR. Primers were designed to yield amplicons of approximately 150-200 bp and with temperatures optimized for use with qPCR. Primers used in qPCR are shown in Table S1. Samples were run on QuantStudio 6 RealTime PCR Machine (Thermo Fisher). qPCR experiments were performed in duplicate with at least two biological replicates. Expression levels were quantified using cycle threshold ( $C_T$ ) and were normalized to 16S rRNA. Differences in gene expression were determined using the  $\Delta\Delta C_T$  method (Pfaffl *et al.*, 2018).

## 2.6 Protein Expression and Purification

A CosR expression vector was constructed using pET-28a (+), an expression plasmid with an IPTG-inducible promoter and an N-terminal 6x-His tag. This was accomplished using primers listed in Table S1 to clone the *cosR* gene into the vector, which had been linearized using XhoI and NcoI. During cloning, a 6x His-tag was added to the C-terminal of CosR, allowing for later purification with a NI-NTA column. This vector was transformed into *E. coli* BL21 DE3, and protein expression induced with 0.5 mM IPTG after growth to mid-exponential phase to confirm production of CosR in this strain. *E. coli* BL21-cosR was then grown aerobically to an  $OD_{600}$  of 0.4, at which point CosR production was induced using IPTG, and allowed to grow for 24 hours, with aeration. Cells were then harvested and lysed using a

microfluidizer. Debris was pelleted through centrifugation at 24,000 x g for 35 mins at 4°C. Clarified supernatant was then loaded onto an IMAC Ni-NTA column equilibrated with a wash buffer containing 50 mM NaPO<sub>4</sub>, 200 mM NaCl, supplemented with 20 mM imidazole buffer and adjusted to pH 7.4. The flowthrough was collected and reloaded onto the column. The column was washed with 20 CV of wash buffer with 20 mM imidazole buffer, 20 column volumes (CV) of the wash buffer with 40 mM imidazole buffer, and 10 CV of the wash buffer with 100 mM imidazole buffer to remove any remaining contaminants. CosR-His was eluted using three CVs of elution buffer comprised of 50 mM NaPO<sub>4</sub>, 200 mM NaCl, 500 mM imidazole. After elution, the samples were allowed to dialyze overnight at 4°C in phosphate buffer to remove any imidazole. 20 µL samples of each supernatant, washes, and elutions, as well as after dialysis were run on an SDS-PAGE gel to confirm presence of our target protein, and to estimate final protein purity.

## **2.7 *E. coli* GFP Reporter Assay.**

A GFP-reporter assay was generated using the *E. coli* strain MKH13 (Haardt *et al.*, 1995). *E. coli* MKH13 lacks many of the genes required for compatible solute uptake and biosynthesis, including *betLAB*, *betT*, *ProU*, and *ProP*. As such it is unable to uptake proline, choline, and glycine betaine, nor can it produce glycine betaine from choline (Haardt *et al.*, 1995). A vector was introduced containing an *ectABCaspK* regulatory region:GFP transcriptional fusion (pRUpectA). The *cosR* gene was then expressed from an IPTG-inducible promoter in the pBBR1MCS expression vector (Fig. 5). Strains were grown over night in LB, washed twice with 1X PBS, then diluted 1:1000 in M9G 1%NaCl. Expression of *cosR* was induced with 0.25 mM IPTG for 20-22 hours. GFP fluorescence was measured with excitation at 385 and emission

at 509 nm in black, clear-bottom 96-well plates. Specific fluorescence was calculated for each sample by normalizing fluorescence intensity to OD. This procedure was repeated for all *E. coli* expression assays.

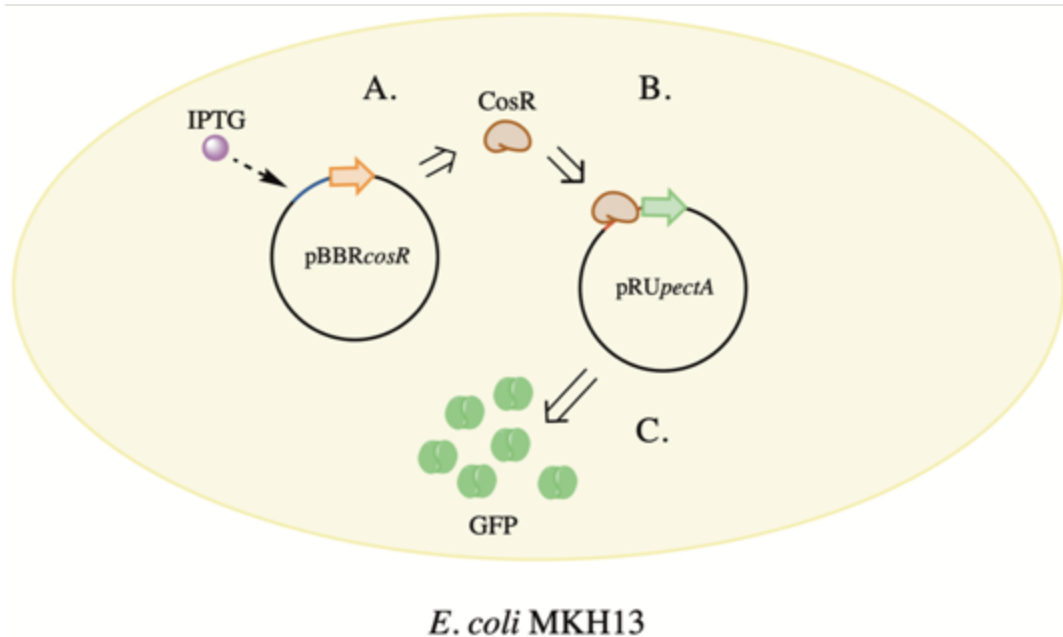


Figure 5. *E. coli* MKH13 GFP-assay. Two plasmids are transformed into this strain. A. The first, shown here as pBBRCosR, encodes the ORF of interest under control of an IPTG-inducible promoter. The addition of IPTG stimulates production of the protein, which is then free to interact with the second vector. B. A second vector encodes a GFP CDS under control of a promoter of interest, in this instance the promoter for the ectoine operon. Transcription from this promoter will produce the GFP protein, which will accumulate in the cell and be quantified after 20 hours of growth.

## 2.8 Electrophoretic Mobility Shift Assay.

DNA fragments were generated from the *ectABCaspK* promoter region using the following primer sets: VPectAFwd/RevA, VPectAFwdB/RevB, VPectAFwdC/Rev (Table S1). The concentration of purified CosR was determined using a Bradford

reagent standard curve, then diluted to the desired concentrations in 1X PBS. The protein was incubated with 36 ng of each DNA fragment in a defined binding buffer (10 mM Tris, 150 mM KCl, 0.5 mM dithiothreitol, 0.1 mM EDTA, 5% polyethylene glycol [PEG] [pH7.4]) (Carpenter *et al.*, 2016). A low-salt (0.5x TBE), 6% native acrylamide gel was pre-run for 2 hours at 4° C (200 V) in 0.5 x TBE buffer. Gels were loaded with the DNA:protein mixtures (10 µL), and run for 2 hours at 4 C (200 V) Finally, gels were stained in an ethidium bromide bath for 20 min and imaged.

## **2.9 Biofilm assay**

Biofilm assays were conducted as previously described (McDonald *et al.*, 2018). Briefly, *V. parahaemolyticus* RIMD2210633 and  $\Delta cosR$  strains were grown statically for 24 hours at 37°C in 96-well polystyrene plates. Following incubation overnight, cultures were removed, and the wells were washed twice with PBS. Crystal violet was added to the wells and allowed incubate for 30 mins, staining any remaining biofilm. The wells were washed once more to remove excess crystal violet, then photographed. The stained biofilm was suspended in DMSO, diluted 1:10, and the OD<sub>595</sub> quantified on a Tecan Plate Reader. Statistical analysis was performed using a student's t-test across two biological replicates.

## Chapter 3

### RESULTS

#### 3.1 *In silico* analysis of *V. parahaemolyticus* CosR

Using the CosR previously described in *V. cholerae* as a seed (Shikuma *et al.*, 2013), a BLAST search was performed on the genome of *V. parahaemolyticus* RIMD2210633. This uncovered a single homologous ORF in the *V. parahaemolyticus* genome, VP1906, that displayed 70% amino acid identity to the CosR of *V. cholerae*. In following the naming convention of *V. cholerae*, we have named the protein encoded by VP1906, CosR. Similar to the gene location in *V. cholerae*, CosR is divergently transcribed from *bcct3* (VP1905).

To determine whether all *V. parahaemolyticus* strains encode this ORF, another BLASTp search was performed using the CosR found in the type strain, against the *V. parahaemolyticus* database. Based on this search, we conclude that CosR is encoded by each of the 874 strains of this species.

#### 3.2 Expression of the Compatible Solute Genes in low salt.

To determine the expression pattern of the ectoine biosynthesis operon in low salt conditions, *V. parahaemolyticus* was grown in minimal media supplemented with glucose (M9G) with optimal salt, 3% NaCl, or low salt, 1% NaCl. Gene expression of the *ectA* and *aspK* was determined using quantitative Real-Time PCR (qPCR) and expressed compared in M9G 1% NaCl compared to M9G 3% NaCl using the  $\Delta\Delta C_T$  method. Expression of *ectA* and *aspK* were found to be 800-fold and 200-fold lower in M9G 1% NaCl, respectively suggesting the *ectABCaspK* biosynthesis operon is regulated by NaCl concentration (Fig. 6).

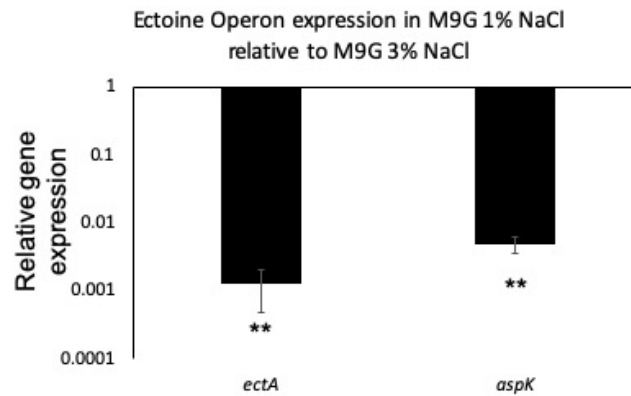


Figure 6. Relative expression of *ectA* and *aspK* in M9G 1% NaCl compared to M9G 3% NaCl in *V. parahaemolyticus* RIMD2210633. Cells were grown to an OD of 0.5, RNA extracted, and qPCR was performed using gene specific primers. Fold changes were calculated using the  $\Delta\Delta C_T$  method and the data was analyzed with a student's t-test.

Next, we analyze expression of the BCCT genes in low versus optimal NaCl conditions. Expression, *bcct1*, *bcct3*, and *bcct4* were significantly repressed in low salt, whereas *bcct2* shows no repression (Fig. 7). Overall the data suggest that both *ect* and *bcct* genes are repressed at low salt conditions.

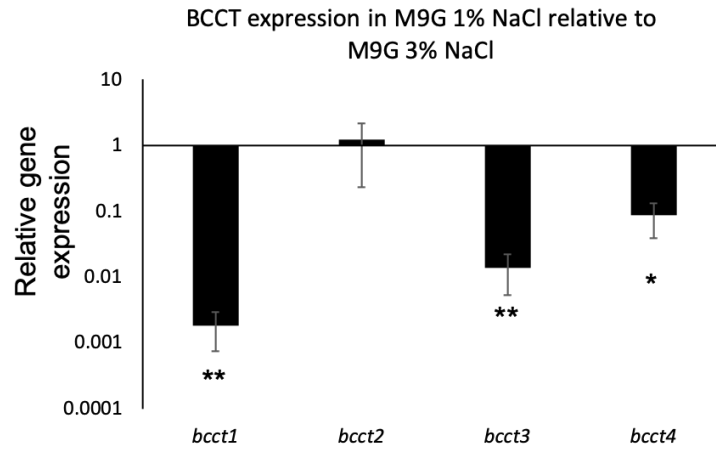


Figure 7. A. Relative expression of *bcct1*, *bcct2*, *bcct3*, and *bcct4* in M9G 1% NaCl compared to M9G 3% NaCl in *V. parahaemolyticus* RIMD2210633. Cells were grown to an OD of 0.5, RNA extracted, and qPCR was performed using gene specific primers. Fold changes were calculated using the  $\Delta\Delta C_T$  method and the data was analyzed with a student's t-test. Depicted is average fold change  $\pm$  1 standard deviation.

To determine whether BCCT expression is impacted by exogenous ectoine, expression of these gene from cells grown in M9G 1% NaCl with ectoine was compared to expression in M9G 1% NaCl. The addition of exogenous ectoine induced *bcct1*, *bcct2*, and *bcct3*, but not *bcct4* (Fig. 8).

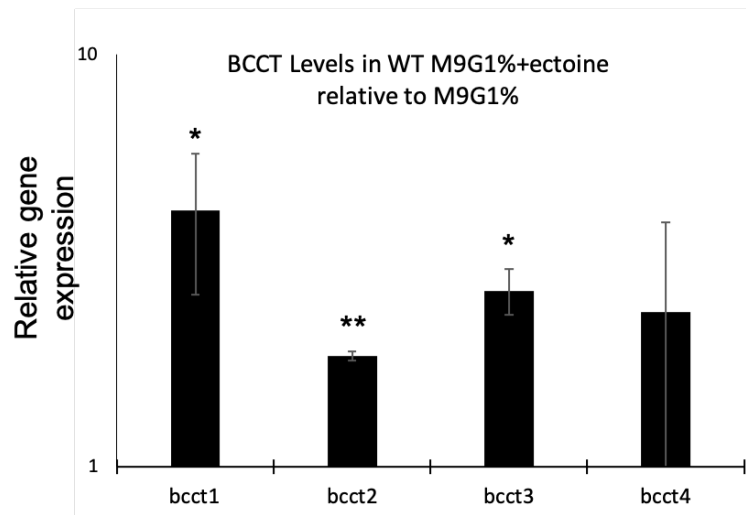


Figure 8. Relative expression of *bcct1*, *bcct2*, *bcct3*, and *bcct4* in M9G 1% NaCl + 100  $\mu$ M ectoine relative to M9G 1% NaCl. Cells were grown to an OD of 0.5, RNA extracted, and qPCR was performed using gene specific primers. Fold changes were calculated using the  $\Delta\Delta C_T$  method and the data was analyzed with a student's t-test. Depicted is average fold change  $\pm$  1 standard deviation.

### 3.3 Growth Analysis of *V. parahaemolyticus* $\Delta cosR$

To determine the role of CosR in *V. parahaemolyticus*, we generated a strain harboring a truncated *cosR* locus. A 417-bp region of the *cosR* genes was deleted, resulting in a  $\Delta cosR$  gene, containing only 60-bp. First, to ensure that the in-frame deletion did not cause any polar effects, the  $\Delta cosR$  strain was grown in LBS and growth over 24 hours was compared to wild type to confirm that no growth defect results from the generation of the mutant (Fig. 9A). As the two strains grew identically, we can be confident that introduction of this truncated ORF had no global effect on growth, and the strain is viable for further use.

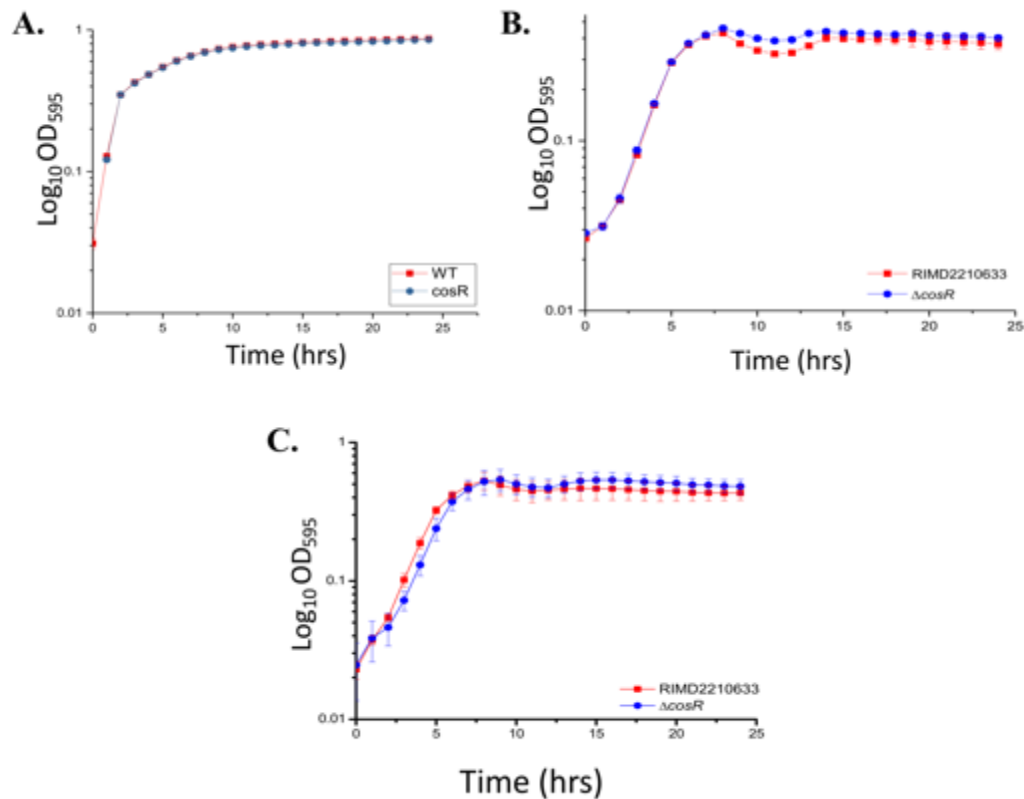


Figure 9. Growth analyses of *V. parahaemolyticus* RIMD2210633 and  $\Delta\text{cosR}$  in A. LBS, B. M9G 1% NaCl), and C. M9G 1% NaCl supplemented with 100  $\mu\text{M}$  ectoine. As the mutant and wild-type strains grow identically,  $\Delta\text{cosR}$  shows no growth defects in any of these media. Growth was analyzed over 24 hours with periodic shaking; each point shown in the average OD  $\pm$  1 standard deviation.

To determine whether the deletion of CosR lead to a growth defect in low salt conditions, growth analysis was examined in M9G 1% NaCl and M9G 1% NaCl supplemented with 100  $\mu\text{M}$  ectoine (Fig. 9B and C). In both growth conditions,  $\Delta\text{cosR}$  grew identically to WT, confirming that there is no defect in the mutant strain. Expression of the *ectABCaspK* genes is regulated by CosR under low salt conditions.

CosR of *V. cholerae*, was shown to repress transcription of the ectoine biosynthesis operon in low salt conditions (Shikuma et al 2013). To assess the role of CosR in the regulation of the ectoine biosynthesis operon in *V. parahaemolyticus*, wild-type (WT) and  $\Delta\text{cosR}$  strains were grown in M9G 1% NaCl to an OD of 0.5. The cells were lysed, RNA was extracted using the Trizol protocol, and cDNA generated. Using primers specific to *ectA* and *aspK*, qPCR was performed on these samples and expression of these genes was normalized to 16S rRNA. Expression of the both genes was significantly increased in  $\Delta\text{cosR}$  as compared to WT (Fig. 10).

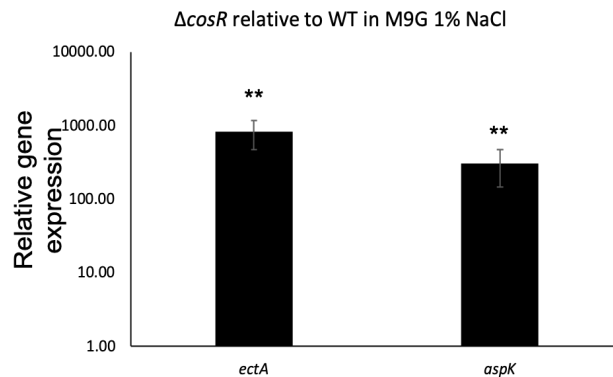


Figure 10. Ectoine operon expression in  $\Delta\text{cosR}$  relative to WT. Fold changes were calculated using the  $\Delta\Delta C_T$  method and the data was analyzed with a student's t-test. Expression of the *ectA* and *aspK* increased 1000-fold and 300-fold, respectively, in the  $\Delta\text{cosR}$  strain. Depicted is average fold change  $\pm 1$  standard deviation.

To determine whether this regulation is a result of CosR directly binding to the promoter region of *ectABCaspK*, we constructed a GFP-reporter assay. In this assay, GFP is placed under the control of a promoter of interest, in this case *PectA*, and CosR is expressed ectopically (Fig. 11). If CosR is able to interact with the promoter, it will

potentially impact the expression of GFP. Relative fluorescence is measured after 20 hours of growth and normalized to OD to obtain specific fluorescence. Specific fluorescence is then compared to a strain not expressing CosR. After 20 hours of growth, specific fluorescence was decreased 3.5-fold in the strain expressing CosR (Fig. 11). This indicates that CosR directly represses transcription of the ectoine operon, and likely binds directly to the ectoine promoter region.

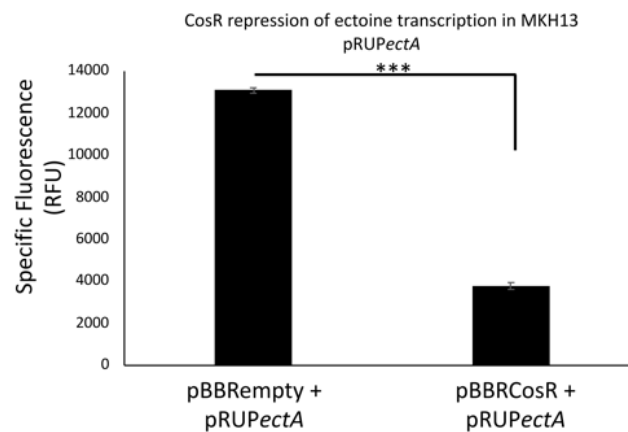


Figure 11. *E. coli* MKH13 strains harboring pBBRCosR+pRUpectA and pBBEmpty+pRUpectA were grown for 20 hours under inducing conditions, at which point specific fluorescence was calculated. *E. coli* MKH13 pBBEmpty+pRUpectA exhibited significantly higher specific fluorescence than *E. coli* MKH13 pBBRCosR+pRUpectA. Statistical analysis was conducted using a student's t-test across two replicates. Depicted is average specific fluorescence  $\pm$  1 standard deviation.

To confirm that CosR binds directly to the promoter of the ectoine biosynthesis operon, we conducted electrophoretic mobility shift assays (EMSAs). The promoter region of the *ectABCaspK* operon was divided into three regions ranging in size from 106 to 137 bp, and named 1A, 1B, and 1C, respectively (Fig. 12A). These fragments

were incubated with purified His-CosR and analyzed on a native 6% acrylamide gel in increasing molar ratios. Shifted bands are indicative of CosR binding to the fragment of interest, and repeating bands could suggest either the presence of multiple binding sites, or the binding of multiple monomers. CosR bound to probes 1A and 1B with a repeating banding pattern, while it did not bind to probe 1C (Fig. 12B). This confirms that CosR binds directly to the promoter region of this operon, likely acting through the formation of a multimeric complex, as is common for MarR type regulators (Alekhun *et al.*, 2001; Hong *et al.*, 2005; Ellison and Miller, 2006; Chang *et al.*, 2010; Perera and Grove, 2010).

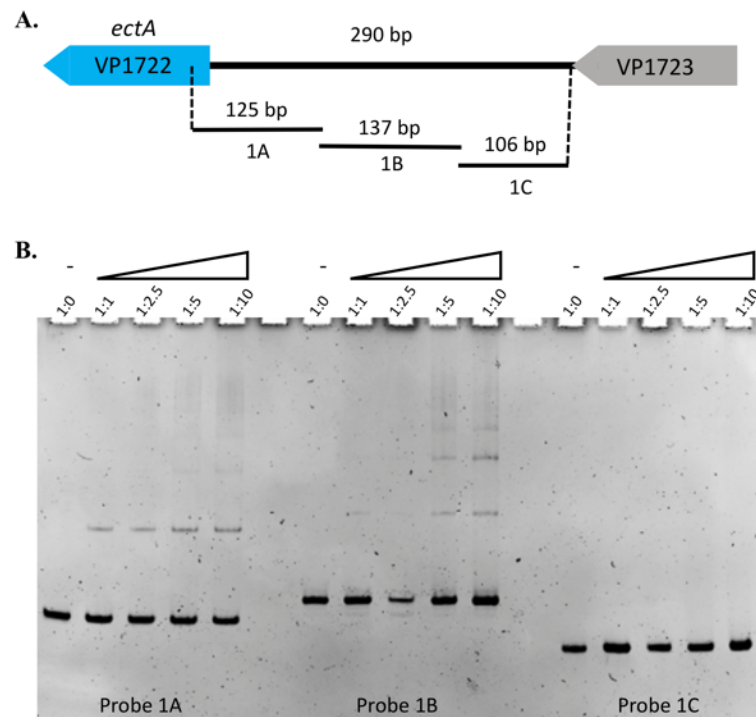


Figure 12. A. A schematic of the probes used for EMSA. The promoter region of *ectABCaspK* was divided into three probes: 1A (125 bp), 1B (137 bp), and 1C (106 bp). Probes 1A and 1B overlap by 25 bp, probes 1B and 1C overlap by 20 bp. B. 36 ng of each probe was incubated with purified His-CosR in varying concentrations from 0 to 0.44  $\mu$ M. The DNA-protein mixtures were run on a 6% native polyacrylamide gel for 2 hr, stained, and imaged.

### 3.4 Expression of *bcct1* and *bcct3* are regulated by CosR in Low Salt Conditions

In addition to regulating the ectoine operon of *V. cholerae*, microarray data suggests that CosR is able to repress transcription of OpuD, a BCCT homolog (Shikuma *et al.*, 2013). To determine whether CosR plays a role in the regulation of the BCCTs encoded by *V. parahaemolyticus*, qPCR analysis was performed on cDNA extracted from WT and  $\Delta$ *cosR* grown in low salt conditions and compared. Expression of *bcct1* (VP0456) and *bcct3* (VP1905) were both highly upregulated in the  $\Delta$ *cosR*

strain, at 156-fold and 35-fold, respectively (Fig. 13). Interestingly, *bcct2* (VP1723) and *bcct4* (VPA0356) showed no change in expression (Fig. 13). Taken together, these data suggest that CosR represses expression of *bcct1* and *bcct3*, but not *bcct2* or *bcct4*.

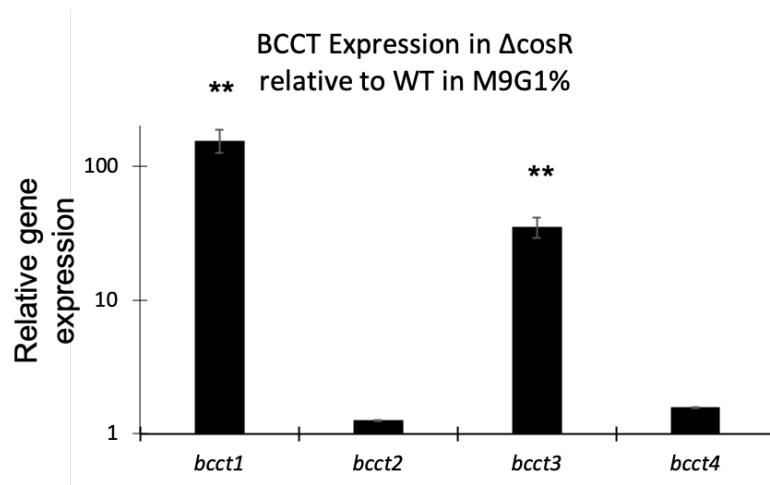


Figure 13. Expression of the *bcct* genes in  $\Delta\text{cosR}$  compared to WT. Strains were grown to an OD of 0.5, RNA extracted, and qPCR was performed using gene specific primers. Fold changes were calculated using the  $\Delta\Delta C_T$  method and the data was analyzed with a student's t-test across two replicates. Depicted is average fold change  $\pm$  1 standard deviation.

To further investigate the role of CosR in the regulation of *bcct1* and *bcct3*, we designed a GFP-reporter assay using the promoter region of each of these genes and examined expression in the presence of ectopically expressed CosR in *E. coli*. Interestingly, there was no significant change in GFP expression of *Pbcct1* between the empty vector and CosR-expressing strains (Fig. 14A), suggesting that CosR may not be the sole low salt regulator of this transporter in *V. parahaemolyticus*, or that CosR requires another factor to repress this gene. CosR did significantly decrease the

level of GFP expression in the *Pbcct3* assay, suggesting that it does directly regulate this gene (Fig. 14B).

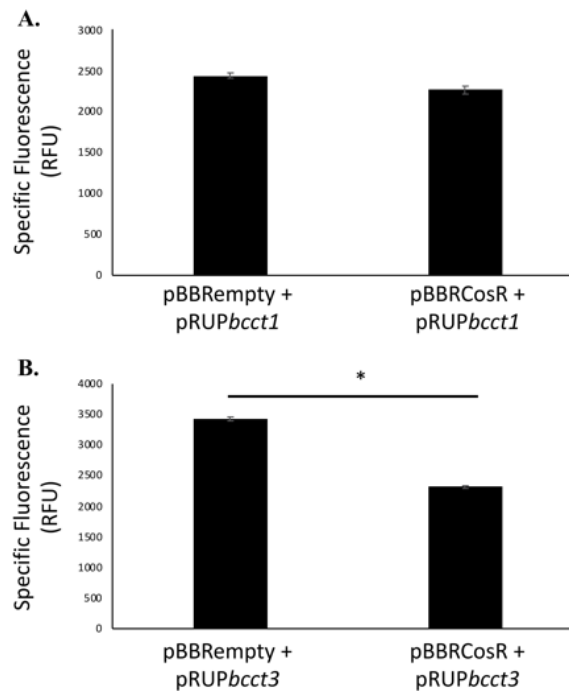


Figure 14. *E. coli* MKH13 strains harboring (A.) pBBRCosR+pRUPbcct1 and pBBREmpty+pRUPbcct1 (B.) pBBRCosR+pRUPbcct3 and pBBREmpty+pRUPbcct3 were grown for 20 hours under inducing conditions, at which point specific fluorescence was calculated. *E. coli* MKH13 pBBREmpty+pRUPbcct1 produced significantly more GFP than *E. coli* MKH13 pBBRCosR+pRUPbcct1. For each, statistical significance was calculated using a student's t-test and the depicted plot shows the average specific fluorescence  $\pm$  1 standard deviation.

Next, we performed EMSAs using the promoter regions of *bcct1* and *bcct3* (Fig. 15A). When incubated with His-CosR, two shifts appear in this probe, however, binding of CosR to this region appears to be weaker than other interactions seen, as

suggested by the intensity of the band. Another EMSA was performed using *Pbcct3* to determine the ability of CosR to bind to this region (Fig. 15B). CosR bound the probe shifted, which at least two times again suggesting that the regulator may bind as a dimer.

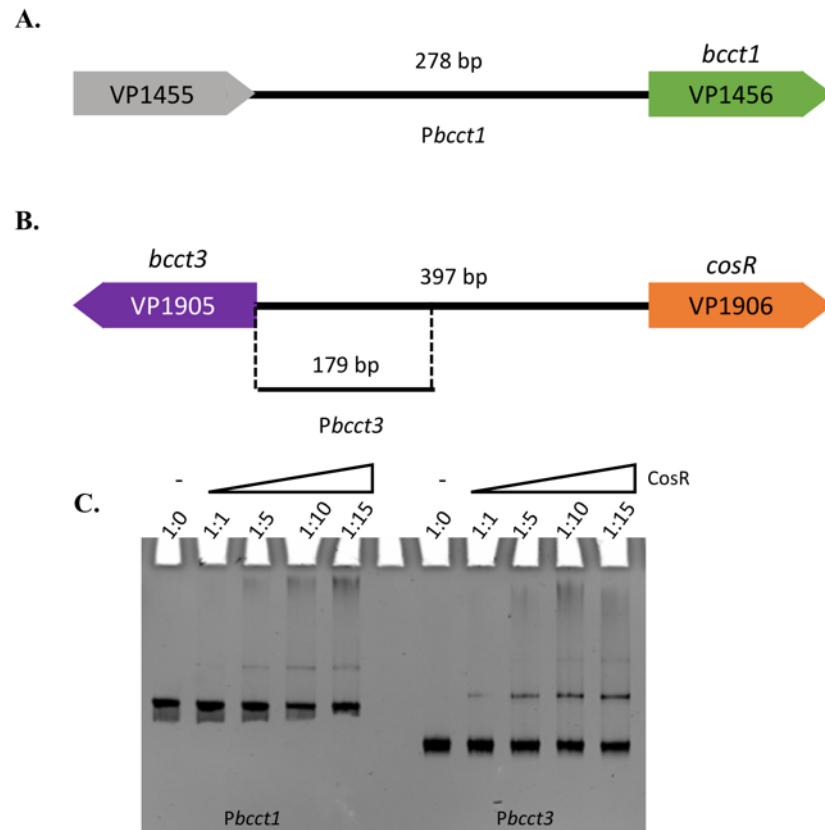


Figure 15. A. The intergenic region immediately upstream of *bcct1* was used for this binding analysis. B. A 179 bp intergenic region upstream of *bcct1*. C. 36 ng of each probe was incubated with purified His-CosR in varying concentrations from 0 to 0.2  $\mu$ M.

### 3.5 CosR expression is independent of salt concentration and does not autoregulate

Expression of the *ectR1* gene encoded by *Methylomicrobium alcaliphilum* 20Z, as well as expression of *cosR* by *V. cholerae*, increased in a salinity dependent manner (Mustakhimov *et al.*, 2010; Shikuma *et al.*, 2013). To determine whether increased salinity increased *cosR* transcripts in *V. parahaemolyticus*, RNA was isolated from cells grown in optimal and low salt conditions and analyzed via qPCR with *cosR* specific probes. Expression of *cosR* was not statistically significant ( $p = 0.08$ ) different between the two conditions, suggesting *cosR* is not regulated by salinity (Fig 16).

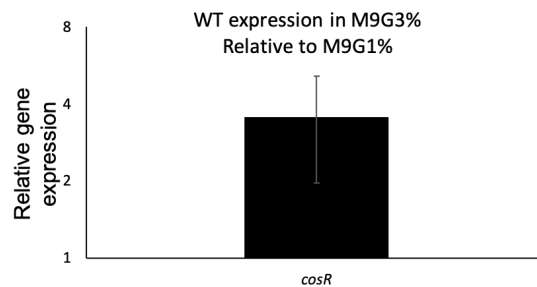


Figure 16. Expression of *cosR* in *V. parahaemolyticus* RIMD2210633 in M9G 3% NaCl relative to M9G 1% NaCl. Cells were grown to an OD of 0.5 in the appropriate media, RNA extracted, and qPCR was performed using gene specific primers. Fold changes were calculated using the  $\Delta\Delta C_T$  method and the data was analyzed with a student's t-test across two replicates. Depicted is average fold change  $\pm$  1 standard deviation.

To determine whether *cosR* expression was dependent on exogenous ectoine, RNA was extracted in both low and optimal salt conditions. RNA from cells grown with exogenous ectoine was compared to those grown without additional ectoine. In low salt conditions, expression of *cosR* in cells grown with ectoine was 0.86-fold lower than those grown without (Fig. 17A). When grown in optimal salt conditions,

*cosR* expression in media supplemented with ectoine was 1.2-fold higher than in cells grown without exogenous ectoine (Fig. 17B). Taken together, these data demonstrate that *cosR* expression is independent of exogenous ectoine in both low and optimal salt conditions.

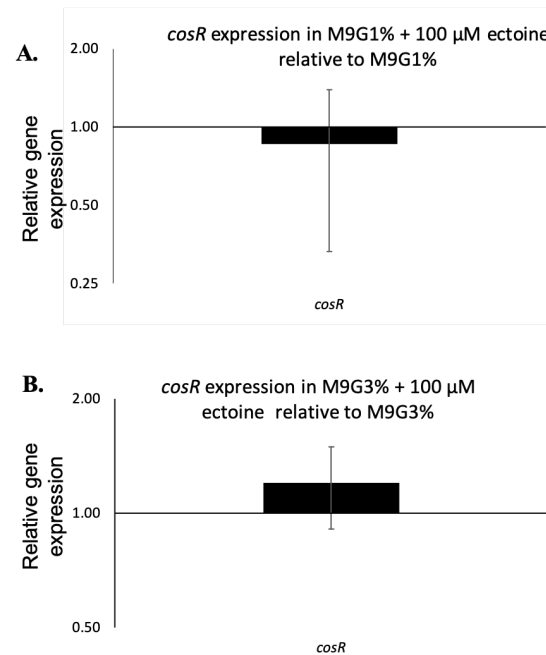


Figure 17. A. Expression of *cosR* in *V. parahaemolyticus* RIMD2210633 in M9G 1% NaCl with 100  $\mu$ M ectoine, relative to M9G 1% NaCl. B. Expression of *cosR* in *V. parahaemolyticus* RIMD2210633 in M9G 3% NaCl with 100  $\mu$ M ectoine, relative to M9G 3% NaCl. Cells were grown to an OD of 0.5 in the appropriate media, RNA extracted, and qPCR was performed using gene specific primers. Fold changes were calculated using the  $\Delta\Delta C_T$  method and the data was analyzed with a student's t-test across two replicates. Depicted is average fold change  $\pm$  1 standard deviation.

A common feature of MarR-type regulators is autoregulation, whereby accumulation of the protein will repress transcription of the gene (Perera and Grove,

2010). To determine whether CosR participates in an autoregulatory loop, two additional *E. coli* GFP-reporter assay strains were constructed: *E. coli* pBBRempty+pRUP*cosR* and *E. coli* pBBRCosR+pRUP*cosR*. Each of these strains harbor a GFP CDS under the control of the *cosR* promoter sequence. These strains were grown for 20 hours in optimal salt minimal media and specific fluorescence calculated. The strain ectopically expressing CosR demonstrated an average specific fluorescence of 2812 RFU. A strain containing harboring only empty vector demonstrated an average specific fluorescence of 4176 RFUs. This difference in GFP production is not statistically significant (Fig. 18).

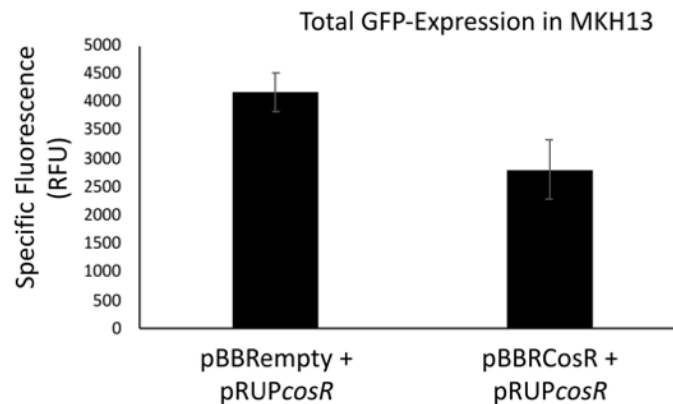


Figure 18. *E. coli* MKH13 strains harboring pBBRCosR+pRUP*cosR* and pBBRempty+pRUP*cosR* were grown for 20 hours under inducing conditions, at which point specific fluorescence was calculated. Statistical significance was calculated using a student's t-test and the depicted plot shows the average specific fluorescence  $\pm$  1 standard deviation.

To determine whether the change in GFP expression was caused by CosR, or other factors in the *E. coli* strain used, as well as if CosR was able to bind to the CosR promoter region, we again conducted an EMSA using a 218-bp probe of this region (Fig. 19AB). CosR was able to bind to this promoter region, though binding began at a higher molar ratio than the other promoters analyzed in this study (Fig. 19B).

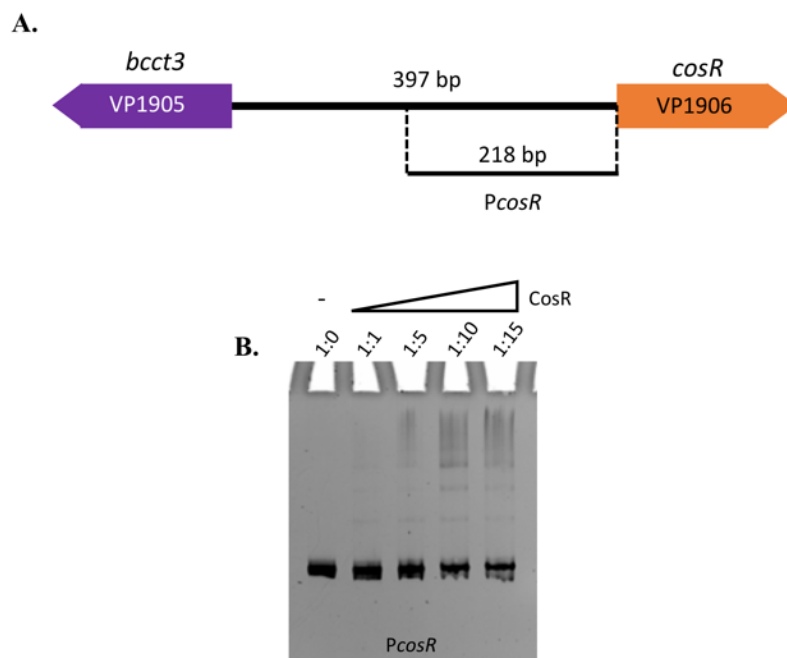


Figure 19. A. A 218 bp intergenic region immediately upstream of *cosR* was used for this binding analysis. B. 36 ng of each probe was incubated with purified His-CosR in varying concentrations from 0 to 0.2  $\mu$ M.

### 3.6 CosR represses biofilm formation

Previously, the CosR was shown to induce the formation of biofilm in stress conditions in *V. cholerae* (Shikuma *et al.*, 2013). To determine whether CosR plays a

similar role in *V. parahaemolyticus*, WT and  $\Delta\text{cosR}$  strains were grown in LBS. After 24 hours of static growth, the culture was removed, loose cells were removed with PBS, and biofilm was stained using crystal violet (Fig. 20A). Biofilm was quantified using OD<sub>595</sub> (Fig. 20B)  $\Delta\text{cosR}$  was found to produce significantly more biofilm than the WT strain ( $p < 0.001$ ), suggesting CosR acts as a repressor of biofilm formation in *V. parahaemolyticus* in optimal salt conditions.

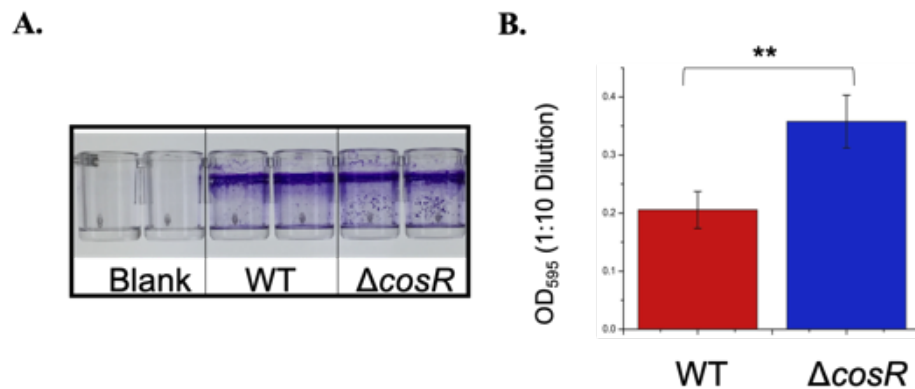


Figure 20. CosR represses biofilm formation in *V. parahaemolyticus*. Biofilms were grown statically at 37 °C for 24 hours. Biofilm was stained with crystal violet, photographed (A), and quantified by determining the OD<sub>595</sub> (B). CosR produced significantly more biofilm than WT ( $p < 0.01$ ).

### 3.7 Distribution of CosR-homologs among the Vibrionaceae

To determine potential targets of CosR regulation in these species, each of the compatible solute systems of *V. parahaemolyticus* were used to identify homologous systems in strains of interest (Table 2). With the exception of *V. sonorensis*, which encodes no compatible solute systems, each of the species analyzed was found to contain at least one BCCT homolog. The majority of species contained at least one

ProU transporter, with the exception of *V. cholerae*, *V. metoecus*, *V. mimicus*, and *Vibrio* sp. RC586, four highly related species. Twenty-eight species encode ectoine biosynthetic genes, while 25 encode a glycine betaine biosynthetic operon.

Table 2. Compatible solute systems identified in select species of Vibrionaceae.

Species	Strain	Transporters			Biosynthetic Operons	
		ProU1	ProU2	BCCT	EctABCAspK	BetIBA
<i>V. parahaemolyticus</i>	RIMD 2210633	+	+	+	+	+
<i>V. campbelli</i>	ATCC BAA116	+	+	+	+	+
<i>V. jasicida</i>	090810c	+	+	+	+	+
<i>V. rotiferianus</i>	B64D1	+	+	+	+	+
<i>V. natriegens</i>	ATCC 14048	+	+	+	+	+
<i>V. diabolicus</i>	FDAARGOS_96	+	+	+	+	+
<i>V. alginolyticus</i>	12G01	+	+	+	+	+
<i>V. alfacensis</i>	CAIM 1831	+	+	+	+	+
<i>V. mytili</i>	CAIM 528	+	-	+	+	+
<i>V. azureus</i>	LC2-005	+	+	+	+	-
<i>V. sagamiensis</i>	NBRC 104589	+	+	+	-	-
<i>V. galathea</i>	S2757	+	+	+	+	+
<i>V. sinaloensis</i>	DSM 21326	+	+	+	-	+
<i>V. pectenocida</i>	CAIM 594	+	+	+	-	+
<i>V. tubiashii</i>	ATCC 19109	+	+	+	+	+
<i>V. caribbeanicus</i>	ATCC BAA-2122	+	+	+	+	+
<i>V. ichthyoenteri</i>	ATCC 700023	+	-	+	+	-
<i>V. panuliri</i>	CAIM 703	+	-	+	+	-
<i>V. nereis</i>	DSM 19584	+	+	+	+	+
<i>V. ponticus</i>	CAIM 1731	+	+	+	+	+
<i>V. salilacus</i>	DSG-S6	+	+	+	+	+
<i>V. sonorensis</i>	CAIM 1076	-	-	-	-	-
<i>V. fluvialis</i>	ATCC 33809	+	+	+	+	+

Species	Strain	ProU1	ProU2	BCCT	EctABCAspK	BetIBA
<i>V. metschnikovii</i>	CIP 69.14	-	+	+	+	+
<i>V. ordalii</i>	ATCC 33509	+	+	+	+	+
<i>A. fischeri</i>	ES114	+	-	+	+	-
<i>V. metoecus</i>	YB5B06	-	-	+	+	-
<i>V. mimicus</i>	ATCC 33654	-	-	+	+	-
<i>V. coralliirubri</i>	MARg	+	+	+	-	+
<i>V. spartinae</i>	CECT 9026	+	+	+	+	+
<i>V. cholerae</i>	N16961	-	-	+	+	-
<i>P. aquimaris</i>	CECT 9191	+	-	+	-	-
<i>V. lentus</i>	5F79	+	+	+	+	+
<i>V. vulnificus</i>	YJ016	-	+	+	-	+
<i>Vibrio sp.</i>	RC586	-	-	+	-	-
<i>P. galathea</i>	S2753	+	+	+	+	+
<i>P. phosphoreum</i>	ANT-2200	+	-	+	-	-

Additionally, seven representative strains were aligned with the EctR1 protein encoded by *Methylomicrobium alcaliphilum* 20Z. The DNA-binding domain defined for EctR1 was labelled, along with all secondary structures, as predicted by Aln2D software (Fig. 21, Mustakhimov et al., 2010). The high conservation of the HTH DNA binding domain, as well as of many of the secondary structures suggest that each of these proteins is likely to function in a similar manner to the CosR described here, as well as the CosR encoded by *V. cholerae*.



## Chapter 4

### DISCUSSION

#### 4.1 CosR regulates elements of the osmotic stress response in *Vibrio parahaemolyticus*

In this study we show that CosR plays a key role in regulating the osmotic stress response of *V. parahaemolyticus* (Fig. 22). In low salt conditions, CosR down-regulates both *bcct1* and *bcct3* as well as *ectABCaspK*, the biosynthetic operon responsible for the *de novo* production of ectoine, and genes involved in biofilm production. For each of these, we have demonstrated that CosR is able to bind to the promoter sequence *in vitro*. Finally, through *in vivo* GFP-assays, we demonstrate that CosR directly represses transcription at the *ectABCaspK* promoter. However, direct repression was not demonstrated *in vitro* for *bcct1* or *bcct3*.

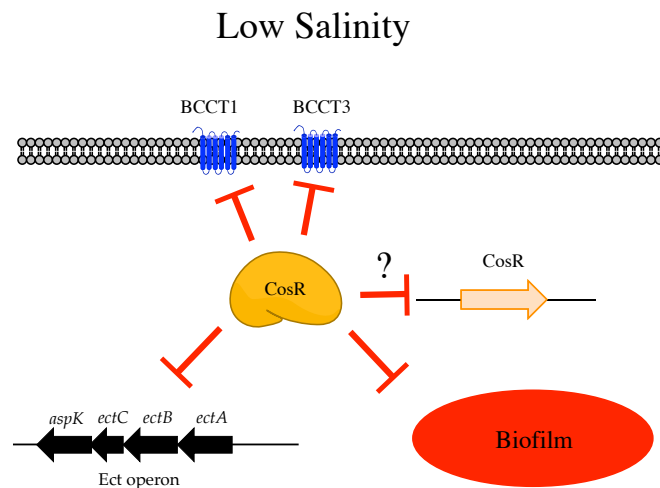


Figure 22. A model of the CosR low salt regulon in *V. parahaemolyticus*. In these conditions, CosR represses transcription of the ectoine operon, as well as *bcct1*, *bcct3*, and genes involved in biofilm formation. Additionally, we demonstrate that CosR likely represses biofilm formation in optimal salt conditions.

This lack of direct repression in our GFP-assay for *bcct1* and *bcct3* could be a result of a number of factors. First, CosR may require other factors in *V. parahaemolyticus* to fully repress transcription from these promoters. Likely, these factors are not present in the *E. coli* genome, and this may explain the lack of repression in this *in vitro* assay. Alternatively, the promoters for the BCCTs may require the action of an activator. Should that be the case, we will not be able to meaningfully quantify the extent of repression by CosR using this assay.

These *in vitro* GFP assays additionally suggest that CosR does not autoregulate, a common feature of many MarR-type regulators (Perera and Grove, 2010). This is exemplified by a number of members of this family but was first identified in the MarR encoded by *E. coli*. This regulator was shown to control both the *marRAB* operon as well as the *marC* gene, which is encoded immediately upstream of and divergently transcribed from *marR* (Martin *et al.*, 1995). MarR was shown to bind twice to two separate palindromic sequences in this intergenic region, thereby repressing transcription of *marRAB* and *marC* (Martin *et al.*, 1995). Other members of this family that are known to autorepress include the MexR found in *Pseudomonas aeruginosa*, and the HpaR repressor of *E. coli* (Evans *et al.*, 2001; Galan *et al.*, 2003). However, a number of MarR-type regulators have been shown not to participate in autoregulation. This includes the *mhqR* and *ohrR* genes *Bacillus subtilis* (Fuangthong *et al.*, 2001; Töwe *et al.*, 2007). We demonstrated that CosR does not bind to its own promoter region in *V. parahaemolyticus*.

#### **4.2 CosR is highly conserved and phylogenetically widespread**

CosR homologs were identified in an additional 37 species across the Vibrionaceae. Strains used in this analysis represent highly divergent species, and

include members of three major genera: *Vibrio*, *Photobacterium*, and *Aliivibrio*. Each of the CosR identified in these species was found to share at least 60% amino acid identity over 100% query cover. In two of these, *V. lentus* and *V. corallirubri*, the CosR-homolog is present downstream of an operon containing the *betIBAchoXWV* ORFs (Appendix Fig. S1B). This region shows amino acid homology to the *betIBAprVWX* operon of *V. parahaemolyticus* (Appendix Fig. S1D). This gene rearrangement suggests that CosR may play an important role in the regulation of both glycine betaine biosynthetic genes, as well as the ChoXWV transporter immediately upstream of this ORF (Appendix Fig. S1D).

In addition, each strain analyzed was searched for each of the compatible solute systems found in *V. parahaemolyticus*. *V. sonorensis* was the only strain which did not show evidence of any compatible solute system homologous to those in *V. parahaemolyticus*. This is likely caused by poor or incomplete genome sequencing.

In *V. parahaemolyticus*, CosR represses the transcription of the ectoine operon, as well as two compatible solute transporters. The high conservation of this protein across *Vibrio* likely indicates that regulation by CosR in this manner will be found in a number of different species. Taken together these data suggest that CosR is an important regulator of compatible solute systems in halophiles.

### 4.3 Future works

This study demonstrates that CosR is an important local regulator of a number of the compatible solute systems encoded by *V. parahaemolyticus*. However, we have yet to investigate the role of CosR in the regulation of the ProU transporters, as well as the glycine betaine operon. Preliminary expression data suggests that CosR likely represses transcription of these genes in low salt conditions also, though we have yet

to demonstrate that CosR is able to bind to these promoters to directly repress transcription.

In addition, we will establish a DNA binding sequence for CosR in *V. parahaemolyticus*. A binding site has been defined for EctR1 in *M. alcaliphilum* 20Z using DNase I foot printing (Mustakhimov *et al.*, 2010). The resulting binding site was an imperfect inverted repeat sequence that is not found in any of the regions to which CosR bound *in vitro* (data not shown). To establish a binding site in *Vibrio*, similar experiments will need to be carried out, though a putative binding site may be predicted as more targets of CosR regulation are discovered in species of interest.

Finally, we will investigate other targets of CosR regulation in *V. parahaemolyticus*. Based on microarray data, the CosR of *V. cholerae*, is able to affect transcription of at least 34 diverse genes (Shikuma *et al.*, 2013). In addition to genes involved in the osmotic stress response, other targets include a number of transporters, cell envelope proteins, amino acid biosynthesis systems, and metabolism, as well as cell motility and biofilm formation (Shikuma *et al.*, 2013). Preliminary data demonstrates that CosR may play similar roles in *V. parahaemolyticus* biofilm formation, though further experimentation is required to fully understand the role of this regulator in these systems.

## REFERENCES

- Alekshun, M. N., Levy, S. B., Mealy, T. R., Seaton, B. A., & Head, J. F. (2001). The crystal structure of MarR, a regulator of multiple antibiotic resistance, at 2.3 Å resolution. *Nature Structural Biology*, 8(8), 710–714.  
<https://doi.org/10.1038/90429>
- Bienert, S., Waterhouse, A., de Beer, T. A. P., Tauriello, G., Studer, G., Bordoli, L., & Schwede, T. (2017). The SWISS-MODEL Repository—new features and functionality. *Nucleic Acids Research*, 45(D1), D313–D319.  
<https://doi.org/10.1093/nar/gkw1132>
- Booth, I. R., & Higgins, C. F. (1990). Enteric bacteria and osmotic stress: Intracellular potassium glutamate as a secondary signal of osmotic stress? *FEMS Microbiology Letters*, 75(2–3), 239–246. <https://doi.org/10.1111/j.1574-6968.1990.tb04097.x>
- Boyd, E. F., Cohen, A. L. V, Naughton, L. M., Ussery, D. W., Binnewies, T. T., Stine, O. C., & Parent, M. A. (2008). Molecular analysis of the emergence of pandemic *Vibrio parahaemolyticus*. In *BMC Microbiol* (Vol. 8, p. 110).  
<https://doi.org/10.1186/1471-2180-8-110>
- Brier, S., Fagnocchi, L., Donnarumma, D., Scarselli, M., Rappuoli, R., Nissum, M., ... Norais, N. (2012). Structural Insight into the Mechanism of DNA-Binding Attenuation of the Neisserial Adhesin Repressor NadR by the Small Natural Ligand 4-Hydroxyphenylacetic Acid. *Biochemistry*, 51(34), 6738–6752.  
<https://doi.org/10.1021/bi300656w>
- Burdette, D. L., Yarbrough, M. L., Orvedahl, A., Gilpin, C. J., & Orth, K. (2008). *Vibrio parahaemolyticus* orchestrates a multifaceted host cell infection by induction of autophagy, cell rounding, and then cell lysis. *Proceedings of the National Academy of Sciences*, 105(34), 12497–12502.  
<https://doi.org/10.1073/pnas.0802773105>
- Bursy, J., Pierik, A. J., Pica, N., & Bremer, E. (2007). Osmotically Induced Synthesis of the Compatible Solute Hydroxyectoine Is Mediated by an Evolutionarily Conserved Ectoine Hydroxylase. *Journal of Biological Chemistry*, 282(43), 31147–31155. <https://doi.org/10.1074/jbc.M704023200>
- Carpenter, M. R., Rozovsky, S., & Boyd, E. F. (2016). Pathogenicity Island Cross Talk Mediated by Recombination Directionality Factors Facilitates Excision from the Chromosome. *Journal of Bacteriology*, 198(5), 766–776.  
<https://doi.org/10.1128/JB.00704-15>

- Cayley, S., Lewis, B. A., Record, M. T., & Jr. (1992). Origins of the osmoprotective properties of betaine and proline in *Escherichia coli* K-12. *Journal of Bacteriology*, *174*(5), 1586–1595. Retrieved from <http://www.ncbi.nlm.nih.gov/pubmed/1537801>
- Chang, Y.-M., Jeng, W.-Y., Ko, T.-P., Yeh, Y.-J., Chen, C. K.-M., & Wang, A. H.-J. (2010). Structural study of TcaR and its complexes with multiple antibiotics from *Staphylococcus epidermidis*. *Proceedings of the National Academy of Sciences*, *107*(19), 8617–8622. <https://doi.org/10.1073/pnas.0913302107>
- Chen, C., & Beattie, G. A. (2007). Characterization of the Osmoprotectant Transporter OpuC from *Pseudomonas syringae* and Demonstration that Cystathionine Synthase Domains Are Required for Its Osmoregulatory Function. *Journal of Bacteriology*, *189*(19), 6901–6912. <https://doi.org/10.1128/JB.00763-07>
- Chen, C., & Beattie, G. A. (2007). Characterization of the Osmoprotectant Transporter OpuC from *Pseudomonas syringae* and Demonstration that Cystathionine- $\beta$ -Synthase Domains Are Required for Its Osmoregulatory Function. *Journal of Bacteriology*, *189*(19), 6901. <https://doi.org/10.1128/JB.00763-07>
- Cohen, S. P., Hächler, H., & Levy, S. B. (1993). Genetic and functional analysis of the multiple antibiotic resistance (mar) locus in *Escherichia coli*. *Journal of Bacteriology*, *175*(5), 1484. Retrieved from <https://www.ncbi.nlm.nih.gov/pmc/articles/PMC193236/?page=1>
- Colwell, R. R. (2006). A Global and Historical Perspective of the Genus *Vibrio*. <https://doi.org/doi:10.1128/9781555815714.ch1>
- Costerton, J. W., Stewart, P. S., & Greenberg, E. P. (1999). Bacterial biofilms: a common cause of persistent infections. *Science*, *284*(5418), 1318–1322. Retrieved from <http://dx.doi.org/>
- Csonka, L. N. (1989). Physiological and genetic responses of bacteria to osmotic stress. *Microbiol Rev*, *53*(1), 121–147. Retrieved from <http://dx.doi.org/>
- Cuthbertson, L., & Nodwell, J. R. (2013). The TetR Family of Regulators. *Microbiol. Mol. Biol. Rev.*, *77*(3), 440–475. <https://doi.org/10.1128/MMBR.00018-13>
- da Costa, M. S., Santos, H., & Galinski, E. A. (1998). An overview of the role and diversity of compatible solutes in Bacteria and Archaea. *Advances in Biochemical Engineering/Biotechnology*, *61*, 117–153. Retrieved from <http://www.ncbi.nlm.nih.gov/pubmed/9670799>

- Dechet, A. M., Yu, P. A., Koram, N., & Painter, J. (2008). Nonfoodborne *Vibrio* Infections: An Important Cause of Morbidity and Mortality in the United States, 1997–2006. *Clinical Infectious Diseases*, 46(7), 970–976. <https://doi.org/10.1086/529148>
- Di Fiore, A., Fiorentino, G., Vitale, R. M., Ronca, R., Amodeo, P., Pedone, C., ... De Simone, G. (2009). Structural Analysis of BldR from *Sulfolobus solfataricus* Provides Insights into the Molecular Basis of Transcriptional Activation in Archaea by MarR Family Proteins. *Journal of Molecular Biology*, 388(3), 559–569. <https://doi.org/10.1016/J.JMB.2009.03.030>
- Eichler, K., Bourgis, F., Buchet, A., Kleber, H. P., & Mandrand-Berthelot, M. A. (1994). Molecular characterization of the *cai* operon necessary for carnitine metabolism in *Escherichia coli*. *Molecular Microbiology*, 13(5), 775–786. Retrieved from <http://www.ncbi.nlm.nih.gov/pubmed/7815937>
- Eitinger, T., Rodionov, D. A., Grote, M., & Schneider, E. (2011). Canonical and ECF-type ATP-binding cassette importers in prokaryotes: diversity in modular organization and cellular functions. *FEMS Microbiology Reviews*, 35(1), 3–67. <https://doi.org/10.1111/j.1574-6976.2010.00230.x>
- Ellison, D. W., & Miller, V. L. (2006). Regulation of virulence by members of the MarR/SlyA family. *Current Opinion in Microbiology*, 9(2), 153–159. <https://doi.org/10.1016/j.mib.2006.02.003>
- Epstein, W. (1986). Osmoregulation by potassium transport in *Escherichia coli*. *FEMS Microbiology Letters*, 39(1–2), 73–78. <https://doi.org/10.1111/j.1574-6968.1986.tb01845.x>
- Eshoo, M. W. (1988). *lac* fusion analysis of the *bet* genes of *Escherichia coli*: regulation by osmolarity, temperature, oxygen, choline, and glycine betaine. *Journal of Bacteriology*, 170(11), 5208–5215. Retrieved from <http://www.ncbi.nlm.nih.gov/pubmed/3141381>
- Evans, K., Adewoye, L., & Poole, K. (2001). MexR Repressor of the *mexAB-oprM* Multidrug Efflux Operon of *Pseudomonas aeruginosa*: Identification of MexR Binding Sites in the *mexA-mexR* Intergenic Region. *Journal of Bacteriology*, 183(3), 807–812. <https://doi.org/10.1128/JB.183.3.807-812.2001>
- Finn, R. D., Mistry, J., Tate, J., Coggill, P., Heger, A., Pollington, J. E., ... Bateman, A. (2010). The Pfam protein families database. *Nucleic Acids Research*, 38. <https://doi.org/10.1093/nar/gkp985>

- Fiorentino, G., Ronca, R., Cannio, R., Rossi, M., & Bartolucci, S. (2007). MarR-Like Transcriptional Regulator Involved in Detoxification of Aromatic Compounds in *Sulfolobus solfataricus*. *Journal of Bacteriology*, *189*(20), 7351–7360. <https://doi.org/10.1128/JB.00885-07>
- Fuangthong, M., Atichartpongkul, S., Mongkolsuk, S., & Helmann, J. D. (2001). OhrR is a repressor of ohrA, a key organic hydroperoxide resistance determinant in *Bacillus subtilis*. *Journal of Bacteriology*, *183*(14), 4134–4141. <https://doi.org/10.1128/JB.183.14.4134-4141.2001>
- FUJINO, T., OKUNO, Y., NAKADA, D., AOYAMA, A., FUKAI, K., MUKAI, T., & UEHO, T. (1953). On the Bacteriological Examination of Shirasu-Food Poisoning. Retrieved from <https://www.cabdirect.org/cabdirect/abstract/19542702324>
- Galan, B., Kolb, A., Sanz, J. M., García, J. L., & Prieto, M. A. (2003). Molecular determinants of the hpa regulatory system of *Escherichia coli*: the HpaR repressor. *Nucleic Acids Research*, *31*(22), 6598–6609. <https://doi.org/10.1093/nar/gkg851>
- Galinski, E. A., & Trüper, H. G. (1994). Microbial behaviour in salt-stressed ecosystems. *FEMS Microbiology Reviews*, *15*(2), 95–108. Retrieved from <https://www.sciencedirect.com/science/article/pii/0168644594901066>
- Gibson, D. G. (2011). Enzymatic Assembly of Overlapping DNA Fragments. In *Methods in enzymology* (Vol. 498, pp. 349–361). <https://doi.org/10.1016/B978-0-12-385120-8.00015-2>
- Gibson, D. G., Young, L., Chuang, R.-Y., Venter, J. C., Hutchison, C. A., & Smith, H. O. (2009). Enzymatic assembly of DNA molecules up to several hundred kilobases. *Nature Methods*, *6*(5), 343–345. <https://doi.org/10.1038/nmeth.1318>
- Gowrishankar, J., & Manna, D. (1996). How is osmotic regulation of transcription of the *Escherichia coli* proU operon achieved? *Genetica*, *97*(3), 363–378. <https://doi.org/10.1007/BF00055322>
- Guex, N., Peitsch, M. C., & Schwede, T. (2009). Automated comparative protein structure modeling with SWISS-MODEL and Swiss-PdbViewer: A historical perspective. *ELECTROPHORESIS*, *30*(S1), S162–S173. <https://doi.org/10.1002/elps.200900140>

- Gul, N., & Poolman, B. (2013). Functional reconstitution and osmoregulatory properties of the ProU ABC transporter from *Escherichia coli*. *Molecular Membrane Biology*, 30(2), 138–148.  
<https://doi.org/10.3109/09687688.2012.754060>
- Haardt, M., Kempf, B., Faatz, E., & Bremer, E. (1995). The osmoprotectant proline betaine is a major substrate for the binding-protein-dependent transport system ProU of *Escherichia coli* K-12. *MGG Molecular & General Genetics*, 246(6), 783–796. <https://doi.org/10.1007/BF00290728>
- Haendiges, J., Rock, M., Myers, R. A., Brown, E. W., Evans, P., & Gonzalez-Escalona, N. (2014). Pandemic *Vibrio parahaemolyticus*, Maryland, USA, 2012. *Emerging Infectious Diseases*, 20(4), 718–720.  
<https://doi.org/10.3201/eid2004.130818>
- Haines-Menges, B., Whitaker, W. B., & Boyd, E. F. (2014). Alternative Sigma Factor RpoE Is Important for *Vibrio parahaemolyticus* Cell Envelope Stress Response and Intestinal Colonization. In *Infect Immun* (Vol. 82, pp. 3667–3677).  
<https://doi.org/10.1128/iai.01854-14>
- Hong, M., Fuangthong, M., Helmann, J. D., & Brennan, R. G. (2005). Structure of an OhrR-ohrA Operator Complex Reveals the DNA Binding Mechanism of the MarR Family. *Molecular Cell*, 20(1), 131–141.  
<https://doi.org/10.1016/J.MOLCEL.2005.09.013>
- Imhoff, J. F. (1986). Osmoregulation and compatible solutes in eubacteria. *FEMS Microbiology Letters*, 39(1–2), 57–66. [https://doi.org/10.1016/0378-1097\(86\)90061-3](https://doi.org/10.1016/0378-1097(86)90061-3)
- Jones, D. T. (1999). Protein secondary structure prediction based on position-specific scoring matrices. *Journal of Molecular Biology*, 292(2), 195–202.  
<https://doi.org/10.1006/JMBI.1999.3091>
- Kalburge, S. S., Carpenter, M. R., Rozovsky, S., Boyd, E. F., & Payne, S. M. (2017). Quorum Sensing Regulators Are Required for Metabolic Fitness in *Vibrio parahaemolyticus*. <https://doi.org/10.1128/IAI.00930-16>
- Kalyuzhnaya, M. G., Khmelenina, V., Eshinimaev, B., Sorokin, D., Fuse, H., Lidstrom, M., & Trotsenko, Y. (2008). Classification of halo(alkali)philic and halo(alkali)tolerant methanotrophs provisionally assigned to the genera *Methylobacterium* and *Methylobacter* and emended description of the genus *Methylobacterium*. *INTERNATIONAL JOURNAL OF SYSTEMATIC AND EVOLUTIONARY MICROBIOLOGY*, 58(3), 591–596.  
<https://doi.org/10.1099/ijs.0.65317-0>

- Kapfhammer, D., Karatan, E., Pflughoeft, K. J., & Watnick, P. I. (2005). Role for glycine betaine transport in *Vibrio cholerae* osmoadaptation and biofilm formation within microbial communities. *Applied and Environmental Microbiology*, *71*(7), 3840–3847. <https://doi.org/10.1128/AEM.71.7.3840-3847.2005>
- Kappes, R. M., Kempf, B., & Bremer, E. (1996). Three transport systems for the osmoprotectant glycine betaine operate in *Bacillus subtilis*: characterization of OpuD. *Journal of Bacteriology*, *178*(17), 5071–5079. Retrieved from <http://www.ncbi.nlm.nih.gov/pubmed/8752321>
- Kempf, B., & Bremer, E. (1998). Uptake and synthesis of compatible solutes as microbial stress responses to high-osmolality environments. *Archives of Microbiology*, *170*(5), 319–330. Retrieved from <http://www.ncbi.nlm.nih.gov/pubmed/9818351>
- Khodr, A., Fairweather, V., Bouffartigues, E., & Rimsky, S. (2015). IHF is a trans-acting factor implicated in the regulation of the proU P2 promoter. *FEMS Microbiology Letters*, *362*(3), 1–6. <https://doi.org/10.1093/femsle/fnu049>
- Kuhlmann, A. U., & Bremer, E. (2002). Osmotically regulated synthesis of the compatible solute ectoine in *Bacillus pasteurii* and related *Bacillus spp.* *Appl Environ Microbiol*, *68*(2), 772–783. Retrieved from <http://dx.doi.org/>
- Kumar, S., Stecher, G., & Tamura, K. (2016). MEGA7: Molecular Evolutionary Genetics Analysis Version 7.0 for Bigger Datasets. *Molecular Biology and Evolution*, *33*(7), 1870–1874. <https://doi.org/10.1093/molbev/msw054>
- Lamark, T., Kaasen, I., Eshoo, M. W., Falkenberg, P., McDougall, J., & Strøm, A. R. (1991). DNA sequence and analysis of the bet genes encoding the osmoregulatory choline-glycine betaine pathway of *Escherichia coli*. *Molecular Microbiology*, *5*(5), 1049–1064. Retrieved from <http://www.ncbi.nlm.nih.gov/pubmed/1956285>
- Lamark, T., Røkenes, T. P., McDougall, J., & Strøm, A. R. (1996). The complex bet promoters of *Escherichia coli*: regulation by oxygen (ArcA), choline (BetI), and osmotic stress. *Journal of Bacteriology*, *178*(6), 1655–1662. Retrieved from <http://www.ncbi.nlm.nih.gov/pubmed/8626294>
- Lanyi, J. K. (1974). Salt-dependent properties of proteins from extremely halophilic bacteria. *Bacteriological Reviews*, *38*(3), 272–290. Retrieved from <http://www.ncbi.nlm.nih.gov/pubmed/4607500>

- Lo, C.-C., Bonner, C. A., Xie, G., D'Souza, M., & Jensen, R. A. (2009). Cohesion Group Approach for Evolutionary Analysis of Aspartokinase, an Enzyme That Feeds a Branched Network of Many Biochemical Pathways. *Microbiology and Molecular Biology Reviews*, 73(4), 594–651. <https://doi.org/10.1128/MMBR.00024-09>
- Louis, P., & Galinski, E. A. (1997). Characterization of genes for the biosynthesis of the compatible solute ectoine from *Marinococcus halophilus* and osmoregulated expression in *Escherichia coli*. *Microbiology*, 143(4), 1141–1149. <https://doi.org/10.1099/00221287-143-4-1141>
- Lucht, J. M., & Bremer, E. (1994). Adaptation of *Escherichia coli* to high osmolarity environments: Osmoregulation of the high-affinity glycine betaine transport system ProU. *FEMS Microbiology Reviews*, 14(1), 3–20. <https://doi.org/10.1111/j.1574-6976.1994.tb00067.x>
- Ma, Y., Wang, Q., Xu, W., Liu, X., Gao, X., & Zhang, Y. (2017). Stationary phase-dependent accumulation of ectoine is an efficient adaptation strategy in *Vibrio anguillarum* against cold stress. *Microbiological Research*, 205, 8–18. <https://doi.org/10.1016/j.micres.2017.08.005>
- Makino, K., Oshima, K., Kurokawa, K., Yokoyama, K., Uda, T., Tagomori, K., ... Iida, T. (2003). Genome sequence of *Vibrio parahaemolyticus*: a pathogenic mechanism distinct from that of *V cholerae*. *The Lancet*, 361(9359), 743–749. [https://doi.org/10.1016/S0140-6736\(03\)12659-1](https://doi.org/10.1016/S0140-6736(03)12659-1)
- Marder, E. P., Cieslak, P. R., Cronquist, A. B., Dunn, J., Lathrop, S., Rabatsky-Ehr, T., ... Geissler, A. L. (2017). Incidence and Trends of Infections with Pathogens Transmitted Commonly Through Food and the Effect of Increasing Use of Culture-Independent Diagnostic Tests on Surveillance — Foodborne Diseases Active Surveillance Network, 10 U.S. Sites, 2013–2016. *MMWR. Morbidity and Mortality Weekly Report*, 66(15), 397–403. <https://doi.org/10.15585/mmwr.mm6615a1>
- Martin, R. G., Nyantakyi, P. S., & Rosner, J. L. (1995). Regulation of the multiple antibiotic resistance (mar) regulon by marORA sequences in *Escherichia coli*. *Journal of Bacteriology*, 177(14), 4176–4178. Retrieved from <http://www.ncbi.nlm.nih.gov/pubmed/7608098>
- McDonald, N. D., DeMeester, K. E., Lewis, A. L., Grimes, C. L., & Boyd, E. F. (2018). Structural and functional characterization of a modified legionaminic acid involved in glycosylation of a bacterial lipopolysaccharide. *The Journal of Biological Chemistry*, 293(49), 19113–19126. <https://doi.org/10.1074/jbc.RA118.004966>

- McDonald, N. D., Regmi, A., Morreale, D. P., Borowski, J. D., Boyd, E. F., & Fidelma Boyd, E. (2019). CRISPR-Cas systems are present predominantly on mobile genetic elements in *Vibrio* species. *BMC Genomics*, *20*(1), 105. <https://doi.org/10.1186/s12864-019-5439-1>
- McLaughlin, J. B., DePaola, A., Bopp, C. A., Martinek, K. A., Napolilli, N. P., Allison, C. G., ... Middaugh, J. P. (2009). Outbreak of *Vibrio parahaemolyticus* Gastroenteritis Associated with Alaskan Oysters. <Http://Dx.Doi.Org/10.1056/NEJMoa051594>. <https://doi.org/NJ200510063531407>
- Meador, C. E., Parsons, M. M., Bopp, C. A., Gerner-Smidt, P., Painter, J. A., & Vora, G. J. (2007). Virulence gene- and pandemic group-specific marker profiling of clinical *Vibrio parahaemolyticus* isolates. *Journal of Clinical Microbiology*, *45*(4), 1133–1139. <https://doi.org/10.1128/JCM.00042-07>
- Merrell, D. S., & Camilli, A. (1999). The *cadA* gene of *Vibrio cholerae* is induced during infection and plays a role in acid tolerance. *Molecular Microbiology*, *34*(4), 836–849. Retrieved from <http://www.ncbi.nlm.nih.gov/pubmed/10564522>
- Mustakhimov, I. I., Reshetnikov, A. S., Glukhov, A. S., Khmelenina, V. N., Kalyuzhnaya, M. G., & Trotsenko, Y. A. (2010). Identification and characterization of EctR1, a new transcriptional regulator of the ectoine biosynthesis genes in the halotolerant methanotroph *Methylomicrobium alcaliphilum* 20Z. *J Bacteriol*, *192*(2), 410–417. <https://doi.org/10.1128/jb.00553-09>
- Nair, G. B., Ramamurthy, T., Bhattacharya, S. K., Dutta, B., Takeda, Y., & Sack, D. A. (2007). Global Dissemination of *Vibrio parahaemolyticus* Serotype O3:K6 and Its Serovariants. In *Clin Microbiol Rev* (Vol. 20, pp. 39–48). American Society for Microbiology Journals. <https://doi.org/10.1128/cmr.00025-06>
- Naughton, L. M., Blumerman, S. L., Carlberg, M., & Boyd, E. F. (2009). Osmoadaptation among *Vibrio* species and unique genomic features and physiological responses of *Vibrio parahaemolyticus*. *Appl Environ Microbiol*, *75*(9), 2802–2810. <https://doi.org/10.1128/aem.01698-08>
- Nigro, O. D., Hou, A., Vithanage, G., Fujioka, R. S., & Steward, G. F. (2011). Temporal and spatial variability in culturable pathogenic *Vibrio spp.* in Lake Pontchartrain, Louisiana, USA, following Hurricanes Katrina and Rita. <https://doi.org/10.1128/AEM.02509-10>

- Nugent, T., & Jones, D. T. (2009). Transmembrane protein topology prediction using support vector machines. *BMC Bioinformatics*, *10*(1), 159.  
<https://doi.org/10.1186/1471-2105-10-159>
- Okuda, J., Ishibashi, M., Hayakawa, E., Nishino, T., Takeda, Y., Mukhopadhyay, A. K., ... Nishibuchi, M. (1997). Emergence of a unique O3:K6 clone of *Vibrio parahaemolyticus* in Calcutta, India, and isolation of strains from the same clonal group from Southeast Asian travelers arriving in Japan. *J Clin Microbiol*, *35*(12), 3150–3155. Retrieved from <http://dx.doi.org/>
- Ongagna-Yhombi, S. Y., & Boyd, E. F. (2013). Biosynthesis of the osmoprotectant ectoine, but not glycine betaine, is critical for survival of osmotically stressed *Vibrio parahaemolyticus* cells. *Appl Environ Microbiol*, *79*(16), 5038–5049.  
<https://doi.org/10.1128/aem.01008-13>
- Ongagna-Yhombi, S. Y., McDonald, N. D., & Boyd, E. F. (2015). Deciphering the Role of Multiple Betaine-Carnitine-Choline Transporters in the Halophile *Vibrio parahaemolyticus*. *Appl Environ Microbiol*, *81*(1), 351–363.  
<https://doi.org/10.1128/aem.02402-14>
- Oren, A. (1999). Bioenergetic aspects of halophilism. *Microbiology and Molecular Biology Reviews : MMBR*, *63*(2), 334–348. Retrieved from <http://www.ncbi.nlm.nih.gov/pubmed/10357854>
- Oren, A. (2008). Microbial life at high salt concentrations: phylogenetic and metabolic diversity. In *Saline Systems* (Vol. 4, p. 2). <https://doi.org/10.1186/1746-1448-4-2>
- Park, K.-S., Ono, T., Rokuda, M., Jang, M.-H., Okada, K., Iida, T., & Honda, T. (2004). Functional characterization of two type III secretion systems of *Vibrio parahaemolyticus*. *Infection and Immunity*, *72*(11), 6659–6665.  
<https://doi.org/10.1128/IAI.72.11.6659-6665.2004>
- Pastor, J. M., Salvador, M., Argandoña, M., Bernal, V., Reina-Bueno, M., Csonka, L. N., ... Cánovas, M. (2010). Ectoines in cell stress protection: Uses and biotechnological production. *Biotechnology Advances*, *28*(6), 782–801.  
<https://doi.org/10.1016/j.biotechadv.2010.06.005>
- Perera, I. C., & Grove, A. (2010). Molecular Mechanisms of Ligand-Mediated Attenuation of DNA Binding by MarR Family Transcriptional Regulators. *Journal of Molecular Cell Biology*, *2*(5), 243–254.  
<https://doi.org/10.1093/jmcb/mjq021>

- Peter, H., Burkovski, A., & Krämer, R. (1996). Isolation, characterization, and expression of the *Corynebacterium glutamicum* betP gene, encoding the transport system for the compatible solute glycine betaine. *Journal of Bacteriology*, 178(17), 5229–5234. Retrieved from <http://www.ncbi.nlm.nih.gov/pubmed/8752342>
- Pfaffl, M. W., of Physiology FML-Weihenstephan, C. of L., & Food Sciences Technical University of Munich, G. (2018). A new mathematical model for relative quantification in real-time RT–PCR. *Nucleic Acids Research*, 29(9). <https://doi.org/10.1093/nar/29.9.e45>
- Philippe, N., Alcaraz, J.-P., Coursange, E., Geiselmann, J., & Schneider, D. (2004). Improvement of pCVD442, a suicide plasmid for gene allele exchange in bacteria. *Plasmid*, 51(3), 246–255. <https://doi.org/10.1016/j.plasmid.2004.02.003>
- Poolman, B., & Glaesker, E. (1998). Regulation of compatible solute accumulation in bacteria. *Molecular Microbiology*, 29(2), 397–407. <https://doi.org/10.1046/j.1365-2958.1998.00875.x>
- Rao, N. V., Shashidhar, R., & Bandekar, J. R. (2013). Comparative analysis of induction of osmotic-stress-dependent genes in *Vibrio vulnificus* exposed to hyper- and hypo-osmotic stress. *Canadian Journal of Microbiology*, 59(5), 333–338. <https://doi.org/10.1139/cjm-2012-0749>
- Record, M. T., Courtenay, E. S., Cayley, D. S., & Guttman, H. J. (1998). Responses of *E. coli* to osmotic stress: large changes in amounts of cytoplasmic solutes and water. *Trends in Biochemical Sciences*, 23(4), 143–148. Retrieved from <http://www.ncbi.nlm.nih.gov/pubmed/9584618>
- Reshetnikov, A. S., Khmelenina, V. N., Mustakhimov, I. I., & Trotsenko, Y. A. (2011). Genes and Enzymes of Ectoine Biosynthesis in Halotolerant Methanotrophs. In *Methods in enzymology* (Vol. 495, pp. 15–30). <https://doi.org/10.1016/B978-0-12-386905-0.00002-4>
- Rhoads, J. (2006). Post–Hurricane Katrina challenge: *Vibrio vulnificus*. *Journal of the American Academy of Nurse Practitioners*, 18, 318–324. <https://doi.org/10.1111/j.1745-7599.2006.00139.x>
- Roberts, M. F. (2004). Osmoadaptation and osmoregulation in archaea: update 2004. *Front Biosci*, 9, 1999–2019. Retrieved from <http://dx.doi.org/>

- Romalde, J. L., de Santiago de Compostela, M., Parasitology CIBUS- Faculty of Biology, C. V. s/n S. de C. 15782 S., [jesus.romalde@usc.es](mailto:jesus.romalde@usc.es), Diéguez, A. L., de Santiago de Compostela, M., ... [sabela.balboa@usc.es](mailto:sabela.balboa@usc.es). (2014). New *Vibrio* species associated to molluscan microbiota: a review. *Frontiers in Microbiology*, 4. <https://doi.org/10.3389/fmicb.2013.00413>
- S Balter, H Hanson, L Kornstein, L Lee, V Reddy, S Sahl, F Stavinsky, M Fage, G Johnson, J Bancroft, W Keene, J Koepsell, M Williams, K MacDonald, N Napolilli, J Hofmann, C Bopp, M Lynch, K Moore, J Painter, N Puhr, P. Y. (2006). *Vibrio parahaemolyticus* Infections Associated with Consumption of Raw Shellfish --- Three States, 2006. Retrieved April 4, 2019, from <https://www.cdc.gov/mmwr/preview/mmwrhtml/mm55d807a1.htm>
- Saridakis, V., Shahinas, D., Xu, X., & Christendat, D. (2008). Structural Insight on the Mechanism of Regulation of the MarR Family of Proteins: High-Resolution Crystal Structure of a Transcriptional Repressor from *Methanobacterium thermoautotrophicum*. *Journal of Molecular Biology*, 377(3), 655–667. <https://doi.org/10.1016/j.jmb.2008.01.001>
- Scholz, A., Stahl, J., de Berardinis, V., Müller, V., & Averhoff, B. (2016). Osmotic stress response in *Acinetobacter baylyi* : identification of a glycine-betaine biosynthesis pathway and regulation of osmoadaptive choline uptake and glycine-betaine synthesis through a choline-responsive BetI repressor. *Environmental Microbiology Reports*, 8(2), 316–322. <https://doi.org/10.1111/1758-2229.12382>
- Schwibbert, K., Marin-Sanguino, A., Bagan, I., Heidrich, G., Lentzen, G., Seitz, H., ... Kunte, H. J. (2011). A blueprint of ectoine metabolism from the genome of the industrial producer *Halomonas elongata* DSM 2581T. *Environmental Microbiology*, 13(8), 1973–1994. <https://doi.org/10.1111/j.1462-2920.2010.02336.x>
- Severin, J., Wohlfarth, A., & Galinski, E. A. (1992). *The predominant role of recently discovered tetrahydropyrimidines for the osmoadaptation of halophilic eubacteria*. *Journal of General Microbiology* (Vol. 54). Retrieved from [www.microbiologyresearch.org](http://www.microbiologyresearch.org)
- Shikuma, N. J., Davis, K. R., Fong, J. N. C., & Yildiz, F. H. (2013). The transcriptional regulator, CosR, controls compatible solute biosynthesis and transport, motility and biofilm formation in *Vibrio cholerae*. *Environmental Microbiology*, 15(5), 1387–1399. <https://doi.org/10.1111/j.1462-2920.2012.02805.x>

- Su, Y. C., & Liu, C. (2007). *Vibrio parahaemolyticus*: a concern of seafood safety. *Food Microbiol*, 24(6), 549–558. <https://doi.org/10.1016/j.fm.2007.01.005>
- Sulavik, M. C., Gambino, L. F., & Miller, P. F. (1995). The MarR Repressor of the Multiple Antibiotic Resistance (mar) Operon in *Escherichia coli*: Prototypic Member of a Family of Bacterial Regulatory Proteins Involved in Sensing Phenolic Compounds. *Molecular Medicine*, 1(4), 436–446. <https://doi.org/10.1007/BF03401581>
- Sutherland, L., Cairney, J., Elmore, M. J., Booth, I. R., & Higgins, C. F. (1986). Osmotic regulation of transcription: induction of the proU betaine transport gene is dependent on accumulation of intracellular potassium. *Journal of Bacteriology*, 168(2), 805–814. <https://doi.org/10.1128/JB.168.2.805-814.1986>
- Thompson, J. D., Higgins, D. G., & Gibson, T. J. (1994). CLUSTAL W: improving the sensitivity of progressive multiple sequence alignment through sequence weighting, position-specific gap penalties and weight matrix choice. *Nucleic Acids Research*, 22(22), 4673–4680. Retrieved from <http://www.ncbi.nlm.nih.gov/pubmed/7984417>
- Töwe, S., Leelakriangsak, M., Kobayashi, K., Van Duy, N., Hecker, M., Zuber, P., & Antelmann, H. (2007). The MarR-type repressor MhqR (YkvE) regulates multiple dioxygenases/glyoxalases and an azoreductase which confer resistance to 2-methylhydroquinone and catechol in *Bacillus subtilis*. *Molecular Microbiology*, 66(1), 40–54. <https://doi.org/10.1111/j.1365-2958.2007.05891.x>
- van Kessel, J. C., Rutherford, S. T., Cong, J.-P. P., Quinodoz, S., Healy, J., Bassler, B. L., ... Bassler, B. L. (2015). Quorum sensing regulates the osmotic stress response in *Vibrio harveyi*. *J Bacteriol*, 197(1), 73–80. <https://doi.org/10.1128/jb.02246-14>
- Vargas, C., Argandona, M., Reina-Bueno, M., Rodriguez-Moya, J., Fernandez-Aunion, C., & Nieto, J. J. (2008). Unravelling the adaptation responses to osmotic and temperature stress in *Chromohalobacter salexigens*, a bacterium with broad salinity tolerance. *Saline Systems*, 4(1), 14. <https://doi.org/10.1186/1746-1448-4-14>
- Vargas, C., Jebbar, M., Carrasco, R., Blanco, C., Calderon, M. I., Iglesias-Guerra, F., & Nieto, J. J. (2006). Ectoines as compatible solutes and carbon and energy sources for the halophilic bacterium *Chromohalobacter salexigens*. *Journal of Applied Microbiology*, 100(1), 98–107. <https://doi.org/10.1111/j.1365-2672.2005.02757.x>

- Ventosa, A., Nieto, J. J., & Oren, A. (1998). Biology of moderately halophilic aerobic bacteria. *Microbiology and Molecular Biology Reviews : MMBR*, 62(2), 504–544. Retrieved from <http://www.ncbi.nlm.nih.gov/pubmed/9618450>
- Vezzulli, L., Grande, C., Reid, P. C., Hélaouët, P., Edwards, M., Höfle, M. G., ... Pruzzo, C. (2016). Climate influence on *Vibrio* and associated human diseases during the past half-century in the coastal North Atlantic. <https://doi.org/10.1073/pnas.1609157113>
- Waterhouse, A., Bertoni, M., Bienert, S., Studer, G., Tauriello, G., Gumienny, R., ... Schwede, T. (2018). SWISS-MODEL: homology modelling of protein structures and complexes. *Nucleic Acids Research*, 46(W1), W296–W303. <https://doi.org/10.1093/nar/gky427>
- Whitaker, W. B., Parent, M. A., Naughton, L. M., Richards, G. P., Blumerman, S. L., & Boyd, E. F. (2010). Modulation of Responses of *Vibrio parahaemolyticus* O3:K6 to pH and Temperature Stresses by Growth at Different Salt Concentrations ▽. In *Appl Environ Microbiol* (Vol. 76, pp. 4720–4729). <https://doi.org/10.1128/aem.00474-10>
- Yancey, P. H. (2004). Compatible and counteracting solutes: protecting cells from the Dead Sea to the deep sea. *Science Progress*, 87(Pt 1), 1–24. Retrieved from <http://www.ncbi.nlm.nih.gov/pubmed/15651637>
- Youssef, N. H., Savage-Ashlock, K. N., McCully, A. L., Luedtke, B., Shaw, E. I., Hoff, W. D., & Elshahed, M. S. (2014). Trehalose/2-sulfotrehalose biosynthesis and glycine-betaine uptake are widely spread mechanisms for osmoadaptation in the Halobacteriales. *The ISME Journal*, 8(3), 636–649. <https://doi.org/10.1038/ismej.2013.165>
- Ziegler, C., Bremer, E., & Krämer, R. (2010). The BCCT family of carriers: from physiology to crystal structure. *Molecular Microbiology*, 78(1), no-no. <https://doi.org/10.1111/j.1365-2958.2010.07332.x>
- Zimmermann, L., Stephens, A., Nam, S.-Z., Rau, D., Kübler, J., Lozajic, M., ... Alva, V. (2018). A Completely Reimplemented MPI Bioinformatics Toolkit with a New HHpred Server at its Core. *Journal of Molecular Biology*, 430(15), 2237–2243. <https://doi.org/10.1016/J.JMB.2017.12.007>

## Appendix

### A.1 Primers Used in this study

Table S1. Primers Used in this Study.

Primer	Sequence (5'-3')	Product size (bp)
<i>Gibson Assembly Primers</i>		
VP1906A	ACCGCATGCGATATCGAGCTTCAAAGCCCCACTTTTGAAC	506
VP1906B	TGATGCTGCCGATAATCGAGACCAATACTTCTTCG	
VP1906C	GGTCTCGATTATCGGCAGCATCACCAAAC	522
VP1906D	GTGGAATTCCCGGAGAGCTCAATCATGAATGGCATCG	
VP1906FLF	CCCATCCAATGCTGTCTTCG	1838
VP1906FLR	CATGCAAGAACGTGTGGAGT	
<i>Protein Purification</i>		
CosR NcoI FWD	TGCCCATGGGTTTGGAAAAGTACGAAGAAGTATTGG	474
CosR XhoI REV	TATCTCGAGTTCTGGTTTGGTGATGCTGCC	
<i>EMSA</i>		
Pbcct1_fwd	tagatagagagagagagagaAAACCGCAAACCTCCCGATC	278
Pbcct1_rev	actcatttttctctctccaCAATCACAAATTTATGCAAAAATGAC	
bcct3 EMSA FWD 2	CGCTTTTTGTAAATGCAAATTACC	179
Pbcct3_rev	actcatttttctctctccaCGTTCCTCTCTATTTTTGTATTATTTTTTC	
cosR EMSA FWD 2	CAAATCTCCACACCATTAATTAG	218
PcosR_rev	actcatttttctctctccaAATTTTTTCATCCAGTCTGTAGG	
ectA FwdA	CCAAGGTGCTGATGTGATCA	125
ectA RevA	CACATTAATCCAGATTAACACGCAG	
ectA FwdB	CTGCGTTTTAATCTGGATTAATGTG	137
ectA RevB	CCCCTGCATTCTGACTCA	
ectA FwdC	ATGAGTCAGAAATGCAGTGGG	106
ectA RevC	GCCACGACGACAAAATAAC	

<b>Primer</b>	<b>Sequence (5'-3')</b>	<b>Product size (bp)</b>
<i>GFP Expression assay</i>		
Pbcct1_fwd	tagatagagagagagagagaAAACCGCAAACCTCCCGATC	278
Pbcct1_rev	actcatttttctctccaCAATCACAAATTTATGCAAAAATGAC	
Pbcct3_fwd	tagatagagagagagagagaAATTTTTTCATCCAGTCTGTAGG	397
Pbcct3_rev	actcatttttctctccaCGTTCCTCTCTATTTTTGTATTATTTTTTC	
PcosR_fwd	tagatagagagagagagagaCGTTCCTCTCTATTTTTGTATTATTTTTTC	397
PcosR_rev	actcatttttctctccaAATTTTTTCATCCAGTCTGTAGG	
PectABC GFP fwd	CTCAAGCTTGTAAGTCGATGCGCCAAC	514
PectABC GFP rev	TATACTAGTATCCTTTGACGTCTAATTAATTTTC	
cosR comp FWD	aggaacaaaagctgggtacTTCCCTACAGACTGGATG	501
cosR comp REV	cggccgctctagaactagtTTATTCTGGTTTGGTGATG	
<i>qPCR</i>		
cosR qPCR F	GCAACTGCGACCACGATTTT	150
cosR qPCR R	GTGTTCTTGCAGCGGAGTTG	
ectA qPCR F	TCGAAAGGGAAGCGCTGAG	125
ectA qPCR R	AGTGCTGACTTGCCATGAT	
aspK qPCR F	CGATGATTCCATTCGCGACG	126
aspK qPCR R	GTCATCTCACTGTAGCCCCG	
bcct1 qPCR F	GTTCCGGTCTTGCGACTTCTC	246
bcct1 qPCR R	CCCATCGCAGTATCAAAGGT	
bcct2 qPCR F	AACAAAGGGTTGCCACTGAC	167
bcct2 qPCR R	TTCAAACCTGTTGCTGCTTG	
bcct3 qPCR F	TGGACGGTATTCTACTGGGC	202
bcct3 qPCR R	CGCCTAACTCGCCTACTTTG	
bcct4 qPCR F	CAAGGCGTAGGCCGATGGT	234
bcct4 qPCR R	ACCGCCCACGATGCTGAACC	
16S F	GGACGGGTGAGTAATGCCTA	193
16S R	CTCAGACCAGCTAGGGATCG	

## A.2 Supplementary Figure 1.

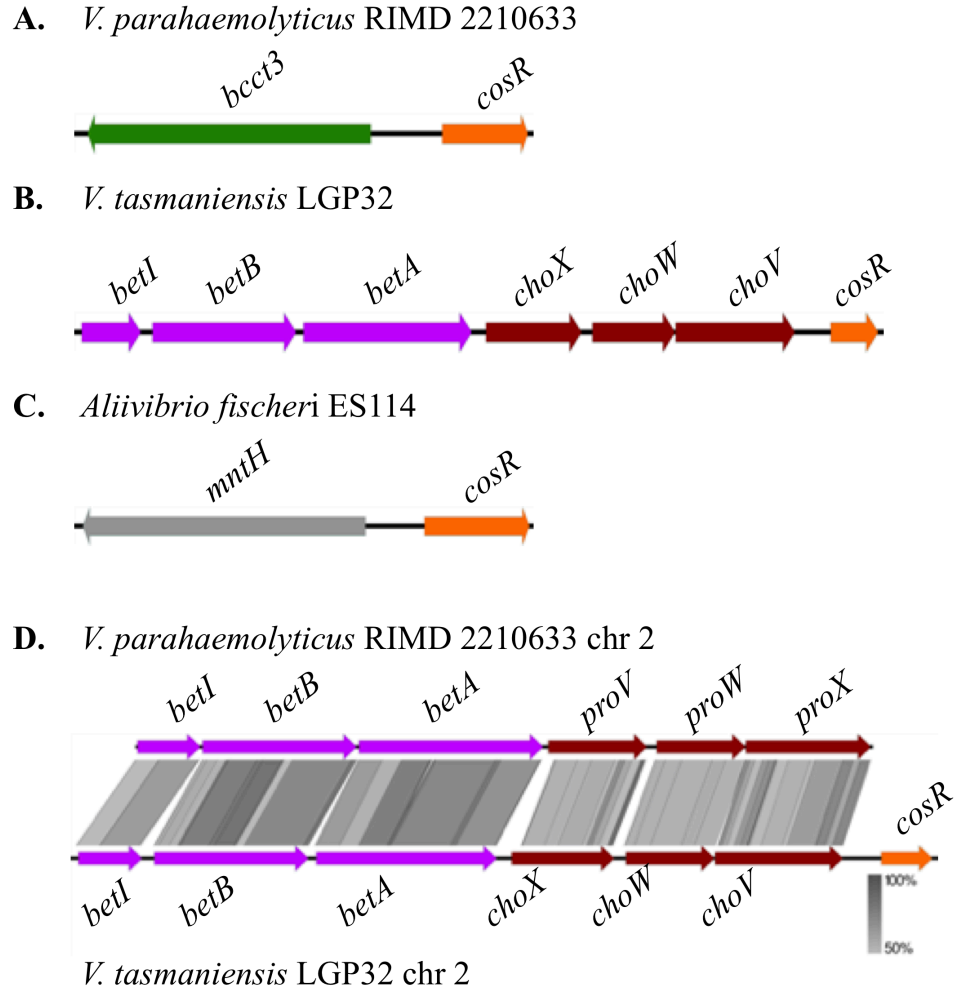


Figure S1. Genomic context of CosR homologs from select Vibrionaceae strains. A. In *V. parahaemolyticus* *cosR* is divergently transcribed from *bcct3* and found on chromosome 1. This structure is well conserved in many *Vibrio* species. B. In *V. tasmaniensis* a CosR homolog is located on chromosome 2, downstream of the *betI**B**A**choX**W**V* operon. C. *A. fischeri* encodes a CosR homolog divergently transcribed from *mntH*, a Mn(II) transport protein. D. The *betI**B**A**proV**W**X* operon of *V. parahaemolyticus* is highly homologous to the *betI**B**A**choX**W**V* operon of *V. tasmaniensis*. Homology was determined with tBLASTx.